FUNCTORIALITY OF COLORED LINK HOMOLOGIES

MICHAEL EHRIG, DANIEL TUBBENHAUER, AND PAUL WEDRICH

ABSTRACT. We prove that the bigraded colored Khovanov–Rozansky type A link and tangle invariants are functorial with respect to link and tangle cobordisms.

CONTENTS

1. INTRODUCTION

Building on Khovanov's categorification of the Jones polynomial [21], Khovanov–Rozansky [25] introduced a link homology theory categorifying the $\mathfrak{sl}_N$ Reshetikhin–Turaev invariant. Their homology theory associates bigraded vector spaces to link diagrams, two of which are isomorphic whenever the diagrams differ only by Reidemeister moves. In the original formulation, the link invariant, thus, takes values in isomorphism classes of bigraded vector spaces.

The first question posed by this construction is whether there is a natural choice of Reidemeister move isomorphisms, such that any isotopy of links in $\mathbb{R}^3$ gives rise to an explicit isomorphism between the Khovanov–Rozansky invariants, which only depends on the isotopy class of the isotopy. A positive answer to this question provides a functor:

$$\left\{ \begin{array}{c} \text{link embeddings in } \mathbb{R}^3 \\ \text{isotopies modulo isotopy} \end{array} \right\} \longrightarrow \left\{ \begin{array}{c} \text{bigraded vector spaces} \\ \text{isomorphisms} \end{array} \right\}$$

The second question, building on the first, is whether this functor can be extended to a functor:

$$\left\{ \begin{array}{c} \text{links embeddings in } \mathbb{R}^3 \\ \text{link cobordisms in } \mathbb{R}^3 \times [0,1] \text{ modulo isotopy} \end{array} \right\} \longrightarrow \left\{ \begin{array}{c} \text{bigraded vector spaces} \\ \text{homogeneous linear maps} \end{array} \right\}$$

The goal of this paper is to answer both questions affirmatively, i.e. to prove the functoriality of Khovanov–Rozansky link homologies for $N \geq 2$ under link cobordisms.

This result is new to the best of our knowledge, except in low-rank cases. For $N = 2$, functorial theories were obtained by Caprau [6], Clark–Morrison–Walker [12] and Blanchet [4] after Khovanov's original theory turned out to have a sign ambiguity, see Jacobsson [19] and Bar-Natan [2]. However, with a bit more care, functoriality can also be achieved in the original construction, see Vogel [46] and joint work with Stroppel [14, 13]. Functoriality for $N = 3$ was proved by Clark [11].

We prove the general functoriality statement in a framework that is different to and more general than Khovanov–Rozansky's construction in [25], as we will now explain.

1.1. **Foams.** Khovanov–Rozansky link homology theories can be defined, or at least described, in many different languages, ranging from those of algebraic geometry, (higher) representation theory and symplectic geometry to those of various incarnations of string theory. The construction most suitable for this paper is combinatorial and uses a graphical calculus of *webs* and *foams*.

Foams play precisely the same role for Khovanov–Rozansky's link homologies that Bar-Natan's cobordisms [2] play for the original Khovanov homology. They can be seen—in a straightforward way—as a categorification of the Murakami–Ohtsuki–Yamada state-sum model [38] for the Reshetikhin–Turaev link invariants of type A, or, equivalently, the graphical calculus for the corresponding representation category, see Cautis–Kamnitzer–Morrison [10].

Foams were first used by Khovanov for the definition of an $\mathfrak{sl}_3$ homology [24], then extended to the higher rank cases by Khovanov–Rozansky [26] and used in the construction of corresponding link homologies by Mackaay–Stošić–Vaz [35].

More recently, Queffelec–Rose [39], building on joint work with Lauda [30] and earlier work of Mackaay and his coauthors [33, 34] on low-rank cases, placed foams in the context of an instance of categorical skew Howe duality. This led to a better understanding of foams as well as a comparison of foam-based link homologies with those obtained via other constructions, see the introduction of Mackaay–Webster [37] for a summary.

A disadvantage of the approach of [39] is that their 2-categories of foams only describe a certain part of the web and foam calculus envisioned by Khovanov–Rozansky and Mackaay–Stošić–Vaz. However, Robert–Wagner [42] have closed this gap while maintaining backward compatibility with [39], and we will use their approach for our paper after explaining its essential features in Section 2.3.

1.2. **Tangles and canopolises.** Proving the functoriality of a link homology theory essentially amounts to checking coherence relations between various ways of composing maps associated to Reidemeister moves and other basic link cobordisms that represent isotopic cobordisms. These relations are the *movie moves* as presented by Carter–Saito [8, Chapter 2]. As demonstrated by Bar-Natan [2], it is extremely useful to be able to perform the required computations locally, i.e. in a small portion of the link diagram.

Fortunately, the construction of link homologies via foams immediately extends to the case of tangles and the invariants have essentially tautological planar composition properties. This is captured in Bar-Natan's notions of canopolises (a.k.a. planar algebras in categories) and canopolis morphisms, which we recall in Section 2.2.

A key idea for our paper is Bar-Natan's insight [2, Section 1.1.1] that the canopolis framework allows a low-effort proof of the fact that Khovanov–Rozansky link homologies are functorial up to scalars. This amounts to a significant proof shortcut, as it then only remains to ensure that these scalars are equal to one. However, this is still a formidable challenge.

1.3. **Colors.** The Murakami–Ohtsuki–Yamada state-sum model in fact determines the $\mathfrak{sl}_N$ Reshetikhin–Turaev invariants of links whose components are colored by fundamental representations of quantum $\mathfrak{sl}_N$, i.e. the quantum exterior powers of the usual vector representation. One categorical level up, foams immediately provide an analogous extension of Khovanov–Rozansky's original *uncolored*—i.e. colored only with the vector representation—construction to the colored case. We will work in this generality and record the coloring of tangle components with exterior power representations by remembering only the exterior exponents and placing them as labels next to the respective strands.

Colored Khovanov–Rozansky homologies have been first constructed by Wu [48] and Yonezawa [50] in a technically difficult generalization of the approach in [25]. That their homological invariants can be recovered via foams was proven in full generality by Queffelec–Rose [39].

1.4. **Deformations.** Arguably the most important tool available for studying Khovanov homology is Lee's deformation [31]. While producing uninteresting link invariants on its own, this deformation naturally appears as the limit of a spectral sequence starting at Khovanov homology, which has been used to extract hidden topological information about knots, see e.g. Rasmussen [40].

A key idea for our paper is Blanchet's use of a Lee-type deformation for proving the functoriality of a modified version of Khovanov homology. In [4] he first proved functoriality up to scalars along Bar-Natan's strategy and then computed these scalars—and showed them to be equal to one—by working in the much simpler setting of the deformation. This approach draws on the combinatorial interpretation of Lee's deformation provided by Bar-Natan–Morrison [3].

The Khovanov–Rozansky link homologies of higher rank are subject to an even richer deformation theory, the exploration of which started with the work of Gornik [17] and Mackaay–Vaz [36] in the uncolored case and Wu [49] in the colored case. These deformations were classified in joint work with Rose [43] and used in the proof of a family of physical conjectures about link homologies [47] by the third named author.

In this paper we draw on the deformed foam technology as developed in [43] to provide a functoriality proof for colored Khovanov–Rozansky invariants following Blanchet's strategy.

1.5. **Equivariance.** An important feature in Blanchet's argument is that, if functoriality holds up to scalars, then these scalars can be computed in a Lee-type deformation. To avoid arguing that these scalars are preserved along Lee-type spectral sequences, we will let our invariants take values in a homotopy category of chain complexes and *not* take homology right away. One advantage of this is that the undeformed, colored link invariant, as well as all its deformations, can be obtained as specializations of a

unifying *equivariant* theory. We then prove that the equivariant theory is functorial up to scalars and that all its specializations inherit this property with the same scalars. It then only remains to compute these scalars in the Lee-type deformation, which is significantly simpler.

The first equivariant, or *universal*, link homology can be traced back to Bar-Natan [2] and Khovanov [23] and it encapsulated both Khovanov homology and Lee's deformation. The case $N = 3$ was treated by Mackaay–Vaz [36]. The extension to higher rank is due to Krasner [27] in the uncolored case, and due to Wu [49] in the colored case. The adjective *equivariant* refers to the fact that these link homologies associate GL_N-equivariant cohomology rings of Grassmannians to colored unknots.

Fortunately, the foam technology of Robert–Wagner [42] is already formulated in the necessary generality to be compatible with the equivariant, colored Khovanov–Rozansky link homologies.

1.6. **Integrality.** The foam based link invariants of Mackaay–Stošić–Vaz [35] can be defined integrally and they give rise to integral versions of Khovanov–Rozansky homologies. These invariants take values in bigraded abelian groups rather than vector spaces. Similarly, in the colored case, Queffelec–Rose [39, Proposition 4.10] have observed that their foam-based construction can also be defined over the integers. The same is true for the construction using Robert–Wagner's foams [42].

We have decided to present the results of this paper using the ground ring $\mathbb{C}$. This is for notational convenience as it allows us to treat the canopolis of equivariant foams and all its specializations in the same framework and using the same language. However, with minimal adjustments our proof of functoriality also works over $\mathbb{Z}$, and we will comment on these variations when necessary.

1.7. **Module structure.** The Khovanov–Rozansky homologies of links are modules over cohomology rings of Grassmannians that appear as the invariants of colored unknots. These actions have a natural interpretation using functoriality: Given a basepoint on a colored link, one can place a small unknot of matching color next to the basepoint. This has the effect of tensoring the link invariant with the corresponding cohomology ring. The action of this ring is then determined by the map associated to the cobordism that merges the unknot with the link at the basepoint.

These module structures carry additional information. For example, Hedden–Ni [18] have shown that they enable Khovanov homology to detect unlinks. Furthermore, module structures are important for the comparison with Floer-theoretic link invariants, see for example Baldwin–Levine–Sarkar [1], and the construction of *reduced*, colored Khovanov–Rozansky homologies [47].

1.8. **Outlook.** We finish by commenting on some interesting topics that we will not investigate further in this paper.

First, it is necessary to emphasize that we prove functoriality under link cobordisms modulo isotopies in $\mathbb{R}^3 \times [0, 1]$. It is tempting to view Khovanov–Rozansky homology as an invariant of links in $S^3 = \mathbb{R}^3 \cup \{\infty\}$ and cobordisms in $S^3 \times I$. Indeed, links generically miss the point ∞ and cobordisms between them generically miss $\infty \times [0, 1]$. However, the same is no longer true for isotopies between link cobordisms.

As we have learned from Scott Morrison, proving the functoriality of Khovanov–Rozansky homology in S^3 would require checking only a single type of additional movie move, which however is non-local. Functoriality in S^3 is also the only missing ingredient

for upgrading Khovanov–Rozansky link homologies to invariants of 4-manifolds with links in their boundary.

A second question concerns the functoriality properties of the extension of colored Khovanov–Rozansky link homologies to invariants of tangled webs, embedded in $\mathbb{R}^3$, under foams embedded in $\mathbb{R}^3 \times [0, 1]$ modulo isotopy. Tangled webs can naturally be accommodated in the framework that we use in this paper and foams embedded in 4-space can be encoded as movies of tangled webs. Isotopies of foams are represented by a finite collection of movie moves, see e.g. work of Carter [7]. We expect that the question of functoriality under foams can be investigated similar as in Section 4.

Next, Khovanov–Rozansky homologies can be extended to the case of colorings by other irreducible representations. Using the framework in the present paper, there are at least two distinct ways of doing this. One uses finite resolutions of these representations by fundamental representations and is analogous to Khovanov's construction for $N = 2$ in [22], see also Robert [41] for the case $N = 3$. In the other approach, the invariants for other colors are computed by inserting *infinite twists* into fundamentally colored cables of the original link, see Rozansky [44] for the case of $N = 2$ and Cautis [9] for the general case. For both constructions it is an interesting question whether they satisfy functoriality properties and admit module structures.

Finally, it is tempting to speculate about foam-based constructions of link homology theories that categorify the Reshetikhin–Turaev invariants outside of type A. Our wish list for such constructions includes that they should allow deformations along splittings of the corresponding Dynkin diagram, as it is the case in type A [43]. This might eventually help to prove functoriality properties for link homologies in other types, but more importantly, it gives hints how to construct the necessary foam theories.

Very preliminary results in this direction have been obtained in [15] where a kind of type D foams were constructed using the foams that appear in the present paper for $N = 2$. However, it is not clear whether these foams can be used to define type D link homologies. Even one categorical level down, there are different web calculi outside of type A [28, 45], not all of which are compatible with Reshetikhin–Turaev invariants.

1.9. **Structure of the paper.** In Section 2 we introduce the canopolis of GL_N-equivariant foams by first defining a free canopolis of foams in Section 2.2 and then imposing additional relations in Section 2.3. In Sections 2.4 and 2.5 we collect a number of foam relations, which we need in the proof of functoriality.

In Section 3 we recall the construction of the categorical tangle invariant and study the chain maps induced by Reidemeister moves.

Finally, the functoriality proof in Section 4 is split into the up-to-scalar check in Section 4.2 followed by the computation of the scalars in Section 4.3.

Remark. For the figures in this paper we have chosen colors that can also be distinguished in grayscale print. ▲

2. GL_N-EQUIVARIANT FOAMS

2.1. **Symmetric polynomials.** We start by briefly recalling several notions regarding symmetric polynomials which we will need in this paper.

Let $\mathbb{A}$ be an alphabet of size $|\mathbb{A}| = a$. We denote by $\mathrm{Sym}(\mathbb{A})$ the $\mathbb{C}$-algebra of symmetric polynomials in the alphabet $\mathbb{A}$. Similarly, for alphabets $\mathbb{A}_i$, we denote by $\mathrm{Sym}(\mathbb{A}_1|\cdots|\mathbb{A}_r)$ the $\mathbb{C}$-algebra of polynomials which are symmetric in each alphabet separately. We view these symmetric polynomial rings as being graded by assigning each variable the degree 2.

We denote the jth elementary symmetric polynomials in $\mathbb{A}$ by $\mathrm{e}_j(\mathbb{A})$, and the jth complete symmetric polynomial in $\mathbb{A}$ by $\mathrm{h}_j(\mathbb{A})$. Recall that the first a of either give an algebraically independent set of generators for $\mathrm{Sym}(\mathbb{A})$, i.e.

$$\mathrm{Sym}(\mathbb{A}) \cong \mathbb{C}[\mathrm{e}_1(\mathbb{A}), \ldots, \mathrm{e}_a(\mathbb{A})] \cong \mathbb{C}[\mathrm{h}_1(\mathbb{A}), \ldots, \mathrm{h}_a(\mathbb{A})],$$

and that $\mathrm{e}_j(\mathbb{A}) = 0$ for $j > a$.

Definition 2.1. Let $\mathbb{A}$ and $\mathbb{B}$ be two disjoint alphabets of sizes a and b. The complete symmetric polynomials in the difference of these two alphabets are elements of $\mathrm{Sym}(\mathbb{A}|\mathbb{B})$ given by the generating function:

$$\sum_{k \geq 0} \mathrm{h}_k(\mathbb{A} - \mathbb{B})x^k = \frac{\prod_{B \in \mathbb{B}}(1 - Bx)}{\prod_{A \in \mathbb{A}}(1 - Ax)}.$$

The complete symmetric polynomials in $\mathbb{A}$ are recovered in the special case $\mathbb{B} = \emptyset$, or under the homomorphism setting the variables in $\mathbb{B}$ to zero:

$$\mathrm{h}_k(\mathbb{A}) = \mathrm{h}_k(\mathbb{A} - \emptyset) = \mathrm{h}_k(\mathbb{A} - \mathbb{B})|_{\mathbb{B} \mapsto 0}.$$

Convention 2.2. Let P denote the set of all integer partitions. For $a, b \in \mathbb{Z}_{\geq 0}$ we write $\mathrm{P}(a)$ for the set of partitions with at most a parts, and $\mathrm{P}(a, b)$ for the set of partitions with at most a parts, all of which are of size at most b.

Partitions $\alpha = (\alpha_1, \ldots, \alpha_a)$ can be identified with Young diagrams with α_i specifying the numbers of boxes in the ith row. Using this identification, let the total number of boxes be denoted by $|\alpha|$ and let $\overline{\alpha}$ denote the Young diagram obtained by reflecting α along its main diagonal. If it is understood that $\alpha \in \mathrm{P}(a, b)$, we write $\alpha^{\mathrm{c}} \in \mathrm{P}(a, b)$ for the Young diagram of the complement of α, whose rows are given by $\alpha^{\mathrm{c}}_{a+1-j} = b - \alpha_j$ and $\mathrm{box}_{a,b} = \emptyset^{\mathrm{c}}$ for the full box Young diagram. Further, we write $\widehat{\alpha} = \overline{\alpha^{\mathrm{c}}}$ for the transpose of the complement of α.

Here is an illustrative example for $a = 3, b = 4$:

Definition 2.3. Let $\alpha = (\alpha_1, \ldots, \alpha_a) \in P(a)$ be a partition. Then the Schur polynomial corresponding to α in the difference of alphabets $\mathbb{A} - \mathbb{B}$ is given by:

$$s_\alpha(\mathbb{A} - \mathbb{B}) = \det((h_{\alpha_i + j - i}(\mathbb{A} - \mathbb{B}))_{1 \le i, j \le a}).$$

The Schur polynomials in $\mathbb{A}$ are recovered in the special case $\mathbb{B} = \emptyset$ or under the homomorphism setting the variables in $\mathbb{B}$ to zero:

$$s_\alpha(\mathbb{A}) = s_\alpha(\mathbb{A} - \emptyset) = s_\alpha(\mathbb{A} - \mathbb{B})|_{\mathbb{B} \mapsto 0}. \qquad \blacktriangle$$

Recall that the Schur polynomials s_α for $\alpha \in P(a)$ form a basis for the $\mathbb{C}$-algebra $\mathrm{Sym}(\mathbb{A})$ with structure constants for the multiplication given by the *Littlewood-Richardson coefficients* $c_{\alpha\beta}^\gamma$, see e.g. [32, Section I.5]. This means for $\alpha, \beta \in P(a)$ that

$$s_\alpha s_\beta = \sum_{\gamma \in P(a)} c_{\alpha\beta}^\gamma s_\gamma.$$

Example 2.4. ([49, Section 2.3], and also [29].) Let Gr_a denote the Grassmannian of a-dimensional subspaces in $\mathbb{C}^N$. This carries an action of GL_N and its GL_N-equivariant cohomology can be presented as follows, see e.g. [16, Lectures 6 and 7]:

$$H^*_{\mathrm{GL}_N}(\mathrm{Gr}_a) \cong \frac{\mathrm{Sym}(\mathbb{A}|\mathbb{S})}{\langle h_{N-a+i}(\mathbb{A} - \mathbb{S}) \mid i > 0\rangle},$$

In fact, $H^*_{\mathrm{GL}_N}(\mathrm{Gr}_a)$ is a graded, free module of rank $\binom{N}{a}$ over the equivariant cohomology of a point $H^*_{\mathrm{GL}_N}(pt)$, which is isomorphic to the symmetric polynomial ring $\mathrm{Sym}(\mathbb{S})$ in an alphabet $\mathbb{S}$ of size N. Moreover, $H^*_{\mathrm{GL}_N}(\mathrm{Gr}_a)$ has a homogeneous bases over $\mathrm{Sym}(\mathbb{S})$ given by the Schur polynomials $s_\alpha(\mathbb{A})$ (or, alternatively, $s_\alpha(\mathbb{A} - \mathbb{S})$) with $\alpha \in P(a, N - a)$.

Let $\mathrm{tr}_a \colon H^*_{\mathrm{GL}_N}(\mathrm{Gr}_a) \to \mathrm{Sym}(\mathbb{S})$ denote the $\mathrm{Sym}(\mathbb{S})$-linear projection onto the $\mathrm{Sym}(\mathbb{S})$-span of the Schur polynomial corresponding to $\mathrm{box}_{a, N-a}(\mathbb{A})$, adjusted by the sign $(-1)^{\binom{a}{2}}$ that we will explain in Remark 2.23. This *trace* satisfies

$$(2.1) \qquad \mathrm{tr}_a(s_\alpha(\mathbb{A}) s_\beta(\mathbb{A} - \mathbb{S})) = (-1)^{\binom{a}{2}} \delta_{\alpha, \beta^c}, \quad \text{for any } \alpha, \beta \in P(a, N - a).$$

This means that it defines a non-degenerate $\mathrm{Sym}(\mathbb{S})$-bilinear form and, thus, a Frobenius algebra structure on $H^*_{\mathrm{GL}_N}(\mathrm{Gr}_a)$. The corresponding (Poincaré) duality maps a basis element $s_\alpha(\mathbb{A})$ to $(-1)^{\binom{a}{2}} s_{\alpha^c}(\mathbb{A} - \mathbb{S})$. $\qquad \blacktriangle$

Example 2.5. ([49, Section 2.3], and also [29].) Let again $\mathbb{A}$ and $\mathbb{B}$ denote alphabets of size a and b. Note that $\mathrm{Sym}(\mathbb{A}|\mathbb{B})$ is a free $\mathrm{Sym}(\mathbb{A} \cup \mathbb{B})$-module of rank $\binom{a+b}{a}$ with homogeneous bases given by the Schur polynomials $s_\alpha(\mathbb{A})$ (or, alternatively, $s_\alpha(\mathbb{A} - \mathbb{B})$) with $\alpha \in P(a, b)$.
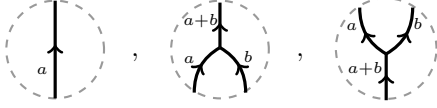
Let $\zeta \colon \mathrm{Sym}(\mathbb{A}|\mathbb{B}) \to \mathrm{Sym}(\mathbb{A} \cup \mathbb{B})$ denote the $\mathrm{Sym}(\mathbb{A} \cup \mathbb{B})$-linear projection onto the $\mathrm{Sym}(\mathbb{A} \cup \mathbb{B})$-span of the Schur polynomial corresponding to $\mathrm{box}_{a, b}(\mathbb{A})$. This map, which is known as the Sylvester operator, is of degree $-2ab$ and satisfies

$$\zeta(s_\alpha(\mathbb{A}) s_\beta(\mathbb{B})) = (-1)^{|\widehat{\alpha}|} \delta_{\alpha, \widehat{\beta}}, \quad \text{for any } \alpha \in P(a, b) \text{ and } \beta \in P(b, a). \qquad \blacktriangle$$

2.2. **Canopolises of webs and foams.** One main toolkit used in this paper is the canopolis formalism introduced by Bar-Natan [2, Section 8.2], which can be seen as a categorification of Jones' planar algebra formalism [20]. We will now describe a canopolis of webs and foams between them.

Throughout this section, let S be a compact, planar surface, i.e. a surface with a fixed embedding into $\mathbb{R}^2$.

Definition 2.6. A web in S is a finite, oriented, trivalent graph, properly embedded in S, together with a labeling of edges by elements of $\mathbb{Z}_{>0}$ satisfying a flow condition at every trivalent vertex. Vertices with incoming labels a, b and outgoing label $a + b$ are called merge vertices, the others split vertices. We illustrate them, and a trivial web, in the case where S is a disk:

(2.2)

▲

For the following definition, let V and W be two webs in S with identical boundary data, i.e. they agree in a collar neighborhood of ∂S.

Definition 2.7. A foam F from V to W is a compact, two-dimensional CW-complex (the particular CW structure on F is irrelevant in the following) with finitely many cells, properly embedded in $S \times [0, 1]$, such that every interior point $x \in F$ has a neighborhood of one of the following three types, which are also illustrated in Figure 2.3.

(I) A smoothly embedded two-dimensional manifold. The connected components of the set of such points are are called the *facets* of F. Each facet is required to be oriented, and we label it with an element of $\mathbb{Z}_{>0}$.

(II) The letter Y (the union of three distinct rays in $\mathbb{R}^2$, meeting in the origin) times $[0, 1]$. The connected components of the set of such singular points are called the *seams* of F. Every seam carries an orientation, which agrees with the orientation induced by two of the adjacents facets, say of label a and b. Then we also require that the third adjacent facet is labeled by $a + b$ and that it induces the opposite orientation on the seam.

(III) The cone on the one-skeleton of a tetrahedron. We call the cone points *singular vertices*, and they are contained in the boundary of precisely four seams and six facets.
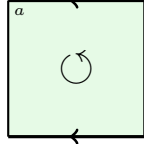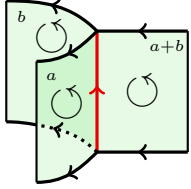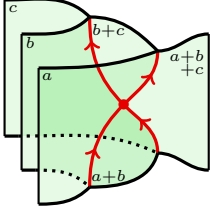
(2.3)   (I):   ,   (II):   ,   (III):

FIGURE 1. Local models and orientation conventions.

Furthermore, $F : V \to W$ is required to satisfy the following conditions:

- The bottom boundary of F in $S \times \{0\}$ agrees with V with matching labels and reversed orientations on the edges. The top boundary of F in $S \times \{1\}$ agrees with W with labels and induced orientations. In particular, singular seams are oriented down through merge vertices and up through split vertices in the boundary webs.
- F restricted to $S \times [0, 1]$ over a collar neighborhood of ∂S is cylindrical, i.e. it agrees with the restriction of $V \times [0, 1]$ to the same set.

We identify foams which differ by an ambient isotopy relative to the boundary in $S \times [0, 1]$. Then the set of webs in S with fixed boundary data assemble into a category with morphisms given by foams mapping from their bottom boundary web to their top boundary web. If S is a disk, we call these *disk categories*. ▲

Remark 2.8. Using classical Morse theory inductively on the skeletons of foams, one can show that one can isotope foams F into generic position so that seams and facets have finitely many non-degenerate critical points for the height function. Then the horizontal slices $F \cap S \times \{z\}$ are webs for all but finitely many $z \in [0, 1]$. See Remark 2.10 for the local foams around these singularities. ▲

Webs in disks carry a natural planar algebra structure. The operations in this planar algebra are given by gluing disks with embedded webs into holed disks with embedded arcs, such that web boundaries are glued in a way that respects the labelings and orientations. An example of a holed disk is given in Figure 2.
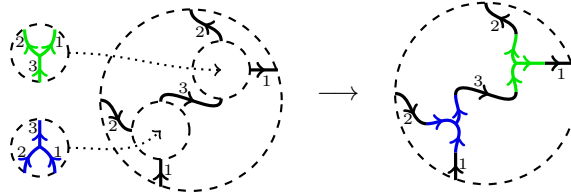
FIGURE 2. Planar composition of webs.

In fact, every web in a disk is generated, in a planar algebra sense, by trivial, merge and split webs as in (2.2).

The planar algebra operations via holed disks immediately extend to planar algebra operations on foams via holed cylindrical foams. Since these operations are compatible with the categorical composition of stacking foams (see e.g. Figure 3), the disk categories assemble into a canopolis in the sense of Bar-Natan [2, Section 8.2].
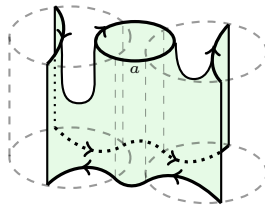
FIGURE 3. Planar algebra composition of two saddles.

Definition 2.9. We denote by **Foam*** the canopolis assembled from the categories of foams over disks, as described above. ▲

Remark 2.10. For a foam in general position, the critical points for the height function have neighborhoods modeled on the following foams.

If the critical point is contained in the interior of a facet, then we get Morse-type handle attachments

(2.4)
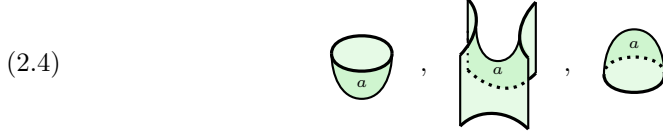
each with two possible orientations. If the critical point is contained in the interior of a seam, then we get the digon creation and annihilation, and zip and unzip foams

(2.5)

(2.6)
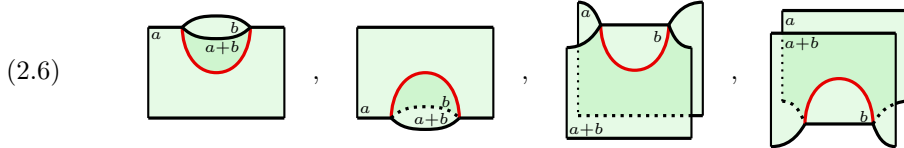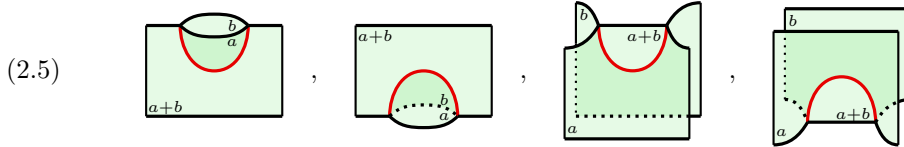
each of which admits two orientations. Finally, singular vertices of the following types appear:

(2.7)
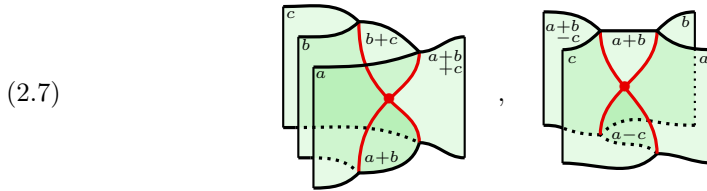
For the rightmost foam we assume that $a > c$. These foams furthermore exist in upside-down versions, and each one admits two orientations.   ▲

We let $\mathbb{Z}\mathbf{Foam}^*$ denote the $\mathbb{Z}$-linear extension of $\mathbf{Foam}^*$ where, additionally, every facet of foams may be decorated by a partition. If gluing two foams results in a foam having two partitions on one facet, it is to be replaced by a $\mathbb{Z}$-linear combination of decorated foams according to a rule modeled on the multiplication of Schur polynomials:

$$\boxed{\begin{matrix} \alpha \\ \beta \end{matrix}} = \sum_{\gamma \in \mathrm{P}(a)} \mathrm{c}_{\alpha\beta}^{\gamma} \boxed{\gamma}$$

Here $\mathrm{c}_{\alpha\beta}^{\gamma}$ are the Littlewood-Richardson coefficients. Using this rule, we will abuse notation and place $\mathbb{Z}$-linear combinations of partitions on foam facets. We also use the interpretation of such linear combinations as symmetric polynomials in an a-element alphabet associated to the facet. This is especially useful when several facets are involved, in which case decorations can be encoded as partially symmetric polynomials.

Definition 2.11. The morphisms in $\mathbb{Z}\mathbf{Foam}^*$ admit a $\mathbb{Z}^2$-grading. The bidegrees of the foam generators in Remark 2.10 are as follows.

  • Cups and caps with label a are of bidegree $(a^2, -a)$.
  • Saddles with label a are of bidegree $(-a^2, a)$.

- Digon creation and annihilation foams of label a and b as in (2.5) are of bidegree $(-ab, 0)$; the ones in (2.6) are of bidegree $(b(a + b), -b)$.
- Zip and unzip foams of label a and b as in (2.5) are of bidegree $(ab, 0)$; the ones in (2.6) are of bidegree $(-b(a + b), b)$.
- The first foam in (2.7) is of bidegree $(0, 0)$, the other one of bidegree $(ab, 0)$.
- A decoration by a partition α is of bidegree $(2|\alpha|, 0)$.

We define the degree $\deg F$ of a foam F in $\mathbb{Z}\mathbf{Foam}^*$ to be the integer obtained by collapsing its bidegree from (k, l) to $k + Nl$.   ▲

Alternatively, the bidegree of a foam can be defined as a weighted Euler characteristic, compare e.g. with [42, Definition 2.3].

For the following definition we consider $H^*_{\mathrm{GL}_N}(pt) \cong \mathrm{Sym}(\mathbb{S})$ as our ground ring. Recall that this ring acts on GL_N-equivariant cohomology in the natural way, see also Example 2.4.

Definition 2.12. Let $\mathbb{S}\mathbf{Foam}^*$ be the additive closure of the $\mathrm{Sym}(\mathbb{S})$-linear, $\mathbb{Z}$-graded canopolis determined by the following data.

- Objects are formal q-degree shifts of webs $q^s V$, where V ranges over the objects of $\mathbb{Z}\mathbf{Foam}^*$, and $s \in \mathbb{Z}$.
- Morphisms are $\mathrm{Sym}(\mathbb{S})$-linear combinations of foams in $\mathbb{Z}\mathbf{Foam}^*$ such that

$$F \colon q^l V \to q^k W \Rightarrow \deg F = k - l.$$

  Hereby we consider the variables of $\mathbb{S}$ to be of degree two.
- Categorical composition is given by the $\mathrm{Sym}(\mathbb{S})$-bilinear extension of the composition in $\mathbb{Z}\mathbf{Foam}^*$.
- Planar composition is given by the $\mathrm{Sym}(\mathbb{S})$-multilinear extension of the planar composition in $\mathbb{Z}\mathbf{Foam}^*$.   ▲

The process of taking the additive closure of a canopolis amounts to allowing formal direct sums of objects as well as matrices of morphisms between them, with composition given by matrix multiplication.

2.3. **The canopolis of GL_N-equivariant foams.** In this section we will describe how to take a quotient of $\mathbb{S}\mathbf{Foam}^*$ that allows the construction of equivariant type A link homologies. The construction uses the foam evaluation of Robert–Wagner [42] to run the *universal construction* as presented by Blanchet–Habegger–Masbaum–Vogel [5] for categories of closed webs and foams between them. Finally, this is extended to the canopolis framework.

2.3.1. *Closed foam evaluation and the universal construction.* The main ingredient that we need is a way of evaluating closed foams. This gives a $\mathrm{Sym}(\mathbb{S})$-linear *evaluation*

$$\mathrm{ev} \colon \mathrm{End}_{\mathbb{S}\mathbf{Foam}^*}(\emptyset) \to \mathrm{Sym}(\mathbb{S}).$$

As our evaluation we choose the GL_N-equivariant version of the explicit and combinatorial evaluation described by Robert–Wagner in [42, Section 2.2] where the reader can find the details. Actually, Robert-Wagner work with torus-equivariant cohomology and thus, with $\mathbb{C}[\mathbb{S}]$ as the ground ring. But this simply amounts to an extension of scalars from $\mathrm{Sym}(\mathbb{S})$.

Remark 2.13. We believe that Robert-Wagner's evaluation coincides (up to minor renormalization details) with the evaluation provided by the Kapustin–Li formula as formulated by Khovanov–Rozansky [26] and used by Mackaay–Stošić–Vaz [35] in the

construction of foam categories and link homologies. We choose to refer to Robert-Wagner because their evaluation is explicit, combinatorial and is already formulated in the equivariant case.   ▲

First, we focus on the disk category with empty boundary in $\mathbb{S}\mathbf{Foam}^*$, i.e. the category of closed webs in the disk and foams between them, which we denote by $\mathbb{S}\mathbf{Foam}^*(\mathrm{cl})$. Since this category is $\mathrm{Sym}(\mathbb{S})$-linear, we can consider the following representable functor to the monoidal category $\mathrm{Sym}(\mathbb{S})$-mod of free $\mathrm{Sym}(\mathbb{S})$-modules:

$$\overline{\mathcal{F}} \colon \mathbb{S}\mathbf{Foam}^*(\mathrm{cl}) \to \mathrm{Sym}(\mathbb{S})\text{-mod},$$
$$V \mapsto \mathrm{Hom}_{\mathbb{S}\mathbf{Foam}^*}(\emptyset, V),$$
$$\left(V \xrightarrow{F} W\right) \mapsto \left(\mathrm{Hom}_{\mathbb{S}\mathbf{Foam}^*}(\emptyset, V) \xrightarrow{F \circ -} \mathrm{Hom}_{\mathbb{S}\mathbf{Foam}^*}(\emptyset, W)\right).$$

The $\mathrm{Sym}(\mathbb{S})$-modules $\overline{\mathcal{F}}(V)$ associated to webs V are too large to be useful. However, given any $G \in \mathrm{Hom}_{\mathbb{S}\mathbf{Foam}^*}(V, \emptyset)$, one considers the map

$$\phi_G \colon \overline{\mathcal{F}}(V) \to \mathrm{Sym}(\mathbb{S}), \quad \phi_G(\emptyset \xrightarrow{F} V) = \mathrm{ev}(G \circ F).$$

This map is well-defined since the evaluation depends only on the combinatorial data of the foams and is, thus, invariant under isotopy. The intersection $\mathcal{I}(V) = \bigcap_G \ker(\phi_G)$ taken over all $G \in \mathrm{Hom}_{\mathbb{S}\mathbf{Foam}^*}(V, \emptyset)$ gives a submodule of $\overline{\mathcal{F}}(V)$. One then sets

$$\mathcal{F}(V) = \overline{\mathcal{F}}(V)/\mathcal{I}(V).$$

We think of $\mathcal{F}(V)$ as the space of all embedded foams with boundary V modulo such $\mathrm{Sym}(\mathbb{S})$-linear combinations that evaluate to zero under arbitrary closures. Naturally, $\mathcal{F}$ extends to a $\mathrm{Sym}(\mathbb{S})$-linear functor

$$\mathcal{F} \colon \mathbb{S}\mathbf{Foam}^*(\mathrm{cl}) \to \mathrm{Sym}(\mathbb{S})\text{-mod}.$$

This might be regarded as a (singular) TQFT for the category of closed webs and foams between them.

In the following we collect some useful properties, which are implicit in [42, Section 3]:

- $\mathcal{F}(\emptyset) \cong \mathrm{Sym}(\mathbb{S})$.
- $\mathcal{F}(V \sqcup W) \cong \mathcal{F}(V) \otimes_{\mathrm{Sym}(\mathbb{S})} \mathcal{F}(W)$.
- The modules $\mathcal{F}(V)$ are free over $\mathrm{Sym}(\mathbb{S})$ with graded rank computed by the MOY-evaluation of webs as in [38].
- $\mathcal{F}$ restricts to a 1+1-dimensional TQFT with values in $\mathrm{Sym}(\mathbb{S})$-mod on the subcategory of $\mathbb{S}\mathbf{Foam}^*(\mathrm{cl})$ consisting of a-labeled 1-manifolds and a-labeled cobordisms between them. This TQFT is determined by the Frobenius algebra given by the GL_N-equivariant cohomology of the Grassmannian Gr_a from Example 2.4.
- The decorations on foam facets are related to basis elements of $H^*_{\mathrm{GL}_N}(\mathrm{Gr}_a)$ via the $\mathrm{Sym}(\mathbb{S})$-linear composite isomorphism

$$\frac{\mathrm{Sym}(\mathbb{A}|\mathbb{S})}{\langle h_{N-a+i}(\mathbb{A} - \mathbb{S}) \mid i > 0 \rangle} \xrightarrow{\cong} H^*_{\mathrm{GL}_N}(\mathrm{Gr}_a) \xrightarrow{\cong} \mathcal{F}(\bigcirc_a),$$

$$s_\alpha(\mathbb{A}) \mapsto \raisebox{-1.2em}{}, \quad \alpha \in \mathrm{P}(a, N-a),$$

where $\bigcirc_a$ denotes the a-labeled circle object.

2.3.2. *Foams modulo relations.* Instead of continuing to work with the functor $\mathcal{F}$, one can form a quotient category of webs and foams, by identifying foams that are sent to equal $\mathrm{Sym}(\mathbb{S})$-linear maps under $\mathcal{F}$. To this end, we define $\mathbb{S}\mathbf{Foam}(\mathrm{cl})$ to be the category with the same objects as $\mathbb{S}\mathbf{Foam}^*(\mathrm{cl})$, but with morphism spaces

$$\mathrm{Hom}_{\mathbb{S}\mathbf{Foam}(\mathrm{cl})}(V, W) = \mathrm{Hom}_{\mathbb{S}\mathbf{Foam}^*(\mathrm{cl})}(V, W)/\ker(\mathcal{F}).$$

We denote the functor induced by $\mathcal{F}$ on $\mathbb{S}\mathbf{Foam}(\mathrm{cl})$ by the same symbol.

The category $\mathbb{S}\mathbf{Foam}(\mathrm{cl})$ is obtained from $\mathbb{S}\mathbf{Foam}^*(\mathrm{cl})$ by imposing the relations in $\ker(\mathcal{F})$. Many of these relations are of a local nature and some important ones are listed in the next section. Before that, however, we would like to extend this quotient to the canopolis framework.

2.3.3. *Canopolization.* Let $F \colon V \to W$ be an arbitrary foam in $\mathbb{S}\mathbf{Foam}^*$ between webs with boundary. Abstractly, F can be considered as a foam from the empty web to the closed web formed by its boundary $\partial F = W \cup_\phi \overline{V}$, which we consider as embedded in a disk. Here $\overline{V}$ denotes the web V reflected in a line and $\cup_\phi$ stands for the planar algebra operation which connects the appropriate boundary points of the webs W and $\overline{V}$. Accordingly, there exist invertible canopolis operations:

$$(2.8) \qquad \mathrm{bend} \colon \mathrm{Hom}_{\mathbb{S}\mathbf{Foam}^*}(V, W) \xrightarrow{\cong} \mathrm{Hom}_{\mathbb{S}\mathbf{Foam}^*}(\emptyset, W \cup_\phi \overline{V}).$$

Informally, such an operation is given by *bending* (or *clapping*) the entire boundary of the foam to the top of the cylinder. In the canopolis, this can be achieved by planar composition with the identity foam on $\overline{V}$ and then pre-composing with a *cup foam* that is obtained by rotating V along a half-circle. The inverse operation is given by bending the part of the boundary down again. These operations are inverse because their composites transform foams only by isotopies. Here is a prototypical example:
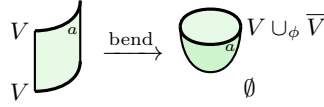
We define

$$\mathcal{I}(V, W) = \mathrm{bend}^{-1}(\mathcal{I}(W \cup_\phi \overline{V})) \subset \mathrm{Hom}_{\mathbb{S}\mathbf{Foam}^*}(V, W).$$

It is easy to see that that the collection of submodules $\mathcal{I}(V, W)$ is preserved under arbitrary canopolis operations in $\mathbb{S}\mathbf{Foam}^*$.

Definition 2.14. Let $\mathbb{S}\mathbf{Foam}$ denote the $\mathrm{Sym}(\mathbb{S})$-linear, $\mathbb{Z}$-graded canopolis obtained as a quotient of the canopolis $\mathbb{S}\mathbf{Foam}^*$ by the canopolis ideal determined by the collection $\mathcal{I}(V, W) \subset \mathrm{Hom}_{\mathbb{S}\mathbf{Foam}^*}(V, W)$. ▲

The subcategory of webs and foams without boundary in $\mathbb{S}\mathbf{Foam}$ is naturally identified with $\mathbb{S}\mathbf{Foam}(\mathrm{cl})$ as introduced above.

Remark 2.15. The graded $\mathrm{Sym}(\mathbb{S})$-rank of the morphism space $\mathrm{Hom}_{\mathbb{S}\mathbf{Foam}}(V, W)$ can be computed via the *bending trick* (2.8) as a rescaled MOY-evaluation of the closed web $W \cup_\phi \overline{V}$. The rescaling depends on the number and labels of critical points introduced in the bending. From this, one can deduce the complex dimensions of the graded components of the morphism spaces in $\mathrm{Hom}_{\mathbb{S}\mathbf{Foam}}(V, W)$. We give some examples that are used later:

- The endomorphism space of a web without vertices, i.e. a trivial tangle, is one-dimensional in degree zero, spanned by the identity foam.
- The morphism spaces between the empty web and a circle of label a are one-dimensional in degree $-a(N-a)$, spanned by the cup and cap foam respectively.
- The morphism spaces between the two distinct webs that consist of two anti-parallel strands of label a are one-dimensional in degree $a(N-a)$, spanned by the saddle foam.   ▲

Remark 2.16. (Integrality.) In fact, the closed foam evaluation of Robert–Wagner takes values in the ring of symmetric polynomials in $\mathbb{S}$ with integer coefficients $\mathrm{Sym}_{\mathbb{Z}}(\mathbb{S})$, see [42, Main Theorem]. Accordingly, all constructions in this section can be performed over the integers as well, and all morphism spaces are free $\mathrm{Sym}_{\mathbb{Z}}(\mathbb{S})$-modules.   ▲

2.4. **GL_N-equivariant foam relations.** Below we collect a number of relations that hold in $\mathbb{S}\mathbf{Foam}$ and that we will need for our main result. In writing these relations we shall decorate foam facets by symmetric polynomials. These correspond to $\mathrm{Sym}(\mathbb{S})$-linear combinations of Schur polynomials, which in turn correspond to partitions. We will switch freely between these conventions.

We start with the following two lemmas, which follow directly from the discussion in Sections 2.3.1 and 2.3.2.

Lemma 2.17. The *neck-cutting* and *sphere relations* hold in $\mathbb{S}\mathbf{Foam}$:

$$(2.9) \qquad \vcenter{\hbox{}} = (-1)^{\binom{a}{2}} \sum_{\alpha \in \mathrm{P}(a,N-a)} \vcenter{\hbox{}} , \quad \vcenter{\hbox{}} = \begin{cases} (-1)^{\binom{a}{2}}, & \text{if } \alpha = \mathrm{box}_{a,N-a}, \\ 0, & \text{otherwise.} \end{cases}$$

In the neck-cutting relations we mean $\mathrm{s}_{\alpha^c} = \mathrm{s}_{\alpha^c}(\mathbb{A}-\mathbb{S})$, but $\mathrm{s}_\alpha = \mathrm{s}_\alpha(\mathbb{B})$, where $\mathbb{A}$ and $\mathbb{B}$ are the alphabet on the cup and cap respectively. The sphere relations are true both for Schur polynomials in $\mathbb{A}$ as well as those in $\mathbb{A}-\mathbb{S}$.   ■

We explain below in Remark 2.23 why the sign $(-1)^{\binom{a}{2}}$ is necessary.

Lemma 2.18. The following relations hold in $\mathbb{S}\mathbf{Foam}$:

$$(2.10) \qquad \vcenter{\hbox{}} = 0, \text{ if } \alpha \notin \mathrm{P}(a,N-a) \text{ or if } a > N.$$

                                                                              ■

Proposition 2.19. The defining relations [39, (3.8) to (3.20)] of the foam 2-category considered by Queffelec-Rose hold in $\mathbb{S}\mathbf{Foam}$.   □

Proof. See [42, Proof of Proposition 4.2].   ■

Example 2.20. We give three examples of relations from Proposition 2.19 that we use later:

$$(2.11) \qquad \vcenter{\hbox{}} = \sum_{\alpha \in \mathrm{P}(a,b)} (-1)^{|\widehat{\alpha}|} \vcenter{\hbox{}}$$

This relation is a special case of [39, (3.14)] in which two facets carry the label zero. This means the corresponding facets are to be erased and their boundary seams to be smoothed out.

The second example illustrates the family of Matveev–Piergallini (MP) relations [39, (3.8)]:

$$(2.12) \qquad \vcenter{\hbox{}} = \vcenter{\hbox{}}$$

Last, the *decoration migration relations* [39, (3.9)], which involve the Littlewood Richardson coefficients:

$$(2.13) \qquad \vcenter{\hbox{}} = \sum_{\alpha,\beta} \mathrm{c}^{\gamma}_{\alpha\beta} \vcenter{\hbox{}}$$

If $\mathbb{A}$, $\mathbb{B}$ and $\mathbb{X}$ are the alphabets on the facets of label a, b and $a+b$ respectively, then this relation identifies symmetric polynomials in $\mathbb{A} \cup \mathbb{B}$ and $\mathbb{X}$. ▲

The Sylvester operator from Example 2.5 allows a compact description of the blister removal relations [39, (3.10)]:

Example 2.21. Let $p \in \mathrm{Sym}(\mathbb{A}|\mathbb{S})$ and $q \in \mathrm{Sym}(\mathbb{B}|\mathbb{S})$ be decorations on the front and rear facets of a blister, respectively. Then we have the following relations in $\mathbb{S}\mathbf{Foam}$:

$$(2.14) \qquad \vcenter{\hbox{}} = \vcenter{\hbox{}} = (-1)^{ab} \vcenter{\hbox{}}$$

▲

Corollary 2.22. Consider the theta foam obtained from the left-hand side of (2.14) by quotienting the boundary of the square to a point. Suppose that this foam carries decorations $p \in \mathrm{Sym}(\mathbb{A}|\mathbb{S})$, $q \in \mathrm{Sym}(\mathbb{B}|\mathbb{S})$ and $r \in \mathrm{Sym}(\mathbb{X}|\mathbb{S})$ on the facets of label a, b and $a+b$. Then this theta foam evaluates to the scalar $\mathrm{tr}_{a+b}(r\zeta(pq)) \in \mathrm{Sym}(\mathbb{S})$ in $\mathbb{S}\mathbf{Foam}$ if we identify symmetric polynomials in $\mathbb{A} \cup \mathbb{B}$ and $\mathbb{X}$ via (2.13). ∎

Remark 2.23. Corollary 2.22 and (2.11) explain why the sign in (2.1) and (2.9) is necessary. Using the notation from Corollary 2.22, we can evaluate a theta foam in two different ways:

Thus, taking $p = \emptyset$ and $q = \mathrm{box}_{b,N-b}$ gives

$$\mathrm{tr}_a(\mathrm{box}_{a,N-a})\mathrm{tr}_b(\mathrm{box}_{b,N-b}) = (-1)^{ab}\mathrm{tr}_{a+b}(\mathrm{box}_{a+b,N-a-b}).$$

Hence, fixing $\mathrm{tr}_1(\mathrm{box}_{1,N-1}) = 1$ determines the rest to be as in (2.9).   ▲

Lemma 2.24. The following relations hold in $\mathbb{S}\mathbf{Foam}$ for $a \geq b$:

(2.15)

Here the middle annulus carries the label $a - b$. Similarly in case $b \geq a$, but with swapped orientation on the seams.   □

Proof. We detach the middle facet from the rear facet via (2.11) at the expense of a decoration $\sum_{\alpha \in \mathrm{P}(a-b,b)}(-1)^{|\widehat{\alpha}|}\mathrm{s}_\alpha(\mathbb{X})\mathrm{s}_{\widehat{\alpha}}(\mathbb{B})$, where $\mathbb{X}$ and $\mathbb{B}$ are the alphabets on the middle and rear facets. Removing the blister in the front facet gives zero, unless $\alpha = \mathrm{box}_{a-b,b}$, see (2.14). Hence, only the coefficient $(-1)^{|\widehat{\emptyset}|} = (-1)^{b(a-b)}$ survives.   ■

2.5. **Specializations and their relations.** From now on, we let $\Sigma = \{\lambda_1, \ldots, \lambda_N\}$ be a set of N pairwise different complex numbers and consider the specialization homomorphism of $\mathbb{C}$-algebras

$$\mathrm{sp}^\Sigma \colon \mathrm{Sym}(\mathbb{S}) \to \mathbb{C}, \quad p(\mathbb{S}) \mapsto p(\Sigma).$$

We define the canopolis $\Sigma\mathbf{Foam}$ as the $\mathbb{C}$-linear canopolis obtained from $\mathbb{S}\mathbf{Foam}$ by specializing variables via sp^Σ. The objects in $\Sigma\mathbf{Foam}$ still carry q-degree shifts, but on the level of morphism spaces, the grading is demoted to a filtration. In the following, we abuse notation by writing sp^Σ for the induced $\mathbb{C}$-linear canopolis morphism from $\mathbb{S}\mathbf{Foam}$ to $\Sigma\mathbf{Foam}$, which respects the filtrations. It is clear that $\Sigma\mathbf{Foam}$ satisfies the Σ-specialized versions of the foam relations already listed for $\mathbb{S}\mathbf{Foam}$.

Example 2.25. In the case $N = 2$ and $\Sigma = \{1, -1\}$ the foams in $\Sigma\mathbf{Foam}$ have been used by Blanchet [4, Section 4]. They give rise to a deformed link homology theory that is analogous to Lee's deformation [31] of Khovanov homology.   ▲

Remark 2.26. Specializing all variables in $\mathbb{S}$ not to distinct numbers, but to zero instead, one recovers a canopolis of webs and foams that can be used for the definition of the (non-equivariant) colored Khovanov–Rozansky link homologies. The canopolis $\Sigma\mathbf{Foam}$ can be seen as its *generic* deformation. Deformations obtained as other specializations of the variables in $\mathbb{S}$ have been studied in [43].   ▲

Lemma 2.27. The algebra of decorations on an a-labeled foam facet is the direct sum of one-dimensional summands indexed by a-element subsets $\mathtt{A} \subset \Sigma$. We denote the corresponding idempotents by $\mathbb{1}_{\mathtt{A}}$ and display them as
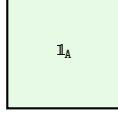
Additionally, decorations $p \in \mathrm{Sym}(\mathbb{A})$ satisfy

$$(2.16) \qquad\qquad p(\mathbb{A}) \cdot \mathbb{1}_{\mathtt{A}} = p(\mathtt{A}) \cdot \mathbb{1}_{\mathtt{A}},$$

i.e. they act on the $\mathtt{A}$-summand via evaluation at $\mathtt{A}$. $\qquad\square$

Here we use that we work over $\mathbb{C}$. However, $\mathbb{Q}$ would suffice as ground ring if $\Sigma \subset \mathbb{Q}$.

Proof. See [43, Lemma 23] and also [43, Proof of Theorem 13]. $\qquad\blacksquare$

Lemma 2.28. ([43, Lemma 23].) Let $\mathtt{A}$, $\mathtt{B}$ and $\mathtt{X}$ subsets of Σ with $|\mathtt{A}| = a$, $|\mathtt{B}| = a$ and $|\mathtt{X}| = a + b$ respectively. Then the following relation holds in $\Sigma\mathbf{Foam}$:

 $= 0,$ unless $\mathtt{A} \cup \mathtt{B} = \mathtt{X}$.

$\qquad\blacksquare$

Lemma 2.29. Let $\mathbb{A}$, $\mathbb{B}$ be alphabets of size a and b respectively. Then we have:

$$r(\mathbb{A}, \mathbb{B}) = \sum_{\alpha \in \mathrm{P}(a,b)} (-1)^{|\widehat{\alpha}|} \mathrm{s}_\alpha(\mathbb{A}) \mathrm{s}_{\widehat{\alpha}}(\mathbb{B}) = \prod_{A \in \mathbb{A}, B \in \mathbb{B}} (A - B).$$

From this we get $r(\mathbb{B}, \mathbb{A}) = (-1)^{ab} r(\mathbb{A}, \mathbb{B})$, and $r(\mathbb{A}, \mathbb{B}) = 0$, if $\mathbb{A} \cap \mathbb{B} \neq \emptyset$. If $\mathbb{X}$ is another alphabet, then $r(\mathbb{A}, \mathbb{B} \cup \mathbb{X}) = r(\mathbb{A}, \mathbb{B}) r(\mathbb{A}, \mathbb{X})$. If $\mathtt{A} \subset \Sigma$, then we also have

$$r(\mathtt{A}, \Sigma \setminus \mathtt{A}) = \sum_{\alpha \in \mathrm{P}(a, N-a)} \mathrm{s}_\alpha(\mathtt{A}) \mathrm{s}_{\alpha^c}(\mathtt{A} - \Sigma) = \sum_{\alpha \in \mathrm{P}(a, N-a)} (-1)^{|\widehat{\alpha}|} \mathrm{s}_\alpha(\mathtt{A}) \mathrm{s}_{\widehat{\alpha}}(\Sigma \setminus \mathtt{A}),$$

which is always non-zero. $\qquad\square$

Proof. For the first equation, see e.g. [32, Section I.4, Example 5]. For the second equation we use $\mathrm{s}_\beta(\mathtt{A} - \Sigma) = (-1)^{|\beta|} \mathrm{s}_{\overline{\beta}}(\Sigma \setminus \mathtt{A})$. $\qquad\blacksquare$

We need to know how idempotent-colored foams behave with respect to the relations found above. We let $r(\mathtt{A}) = (-1)^{\binom{a}{2}} r(\mathtt{A}, \Sigma \setminus \mathtt{A})$.

Lemma 2.30. The following relations hold in $\Sigma\mathbf{Foam}$:

$$(2.17)$$

$\qquad\square$

Proof. The first relation follows from the Σ-specialization of the neck-cutting relation (2.9) combined with (2.16) and Lemma 2.29. The relation for the sphere is obtained by composing both sides of the neck-cutting relation (2.9) with a cap. $\qquad\blacksquare$

Lemma 2.31. The following relation holds in $\Sigma\mathbf{Foam}$:
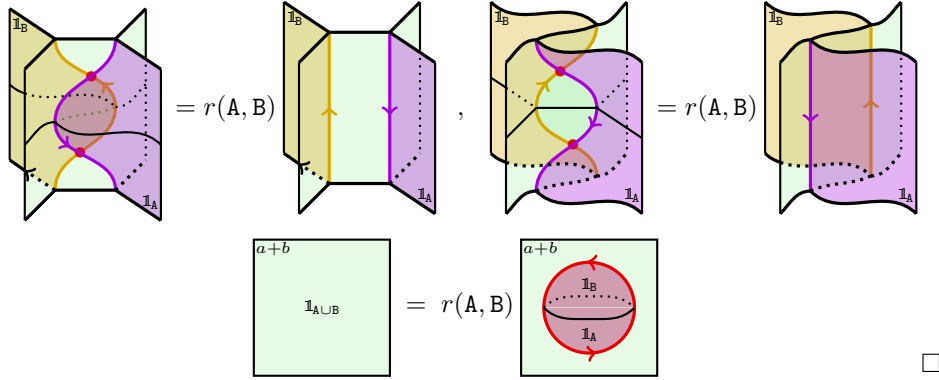
Proof. These relations follow immediately from [39, Relations (3.13) and (3.14)] as well as [43, Relation (4.7)], imported via Proposition 2.19, and (2.16). ∎

Remark 2.32. To reduce the complexity of computations appearing in Section 4, we will use *phase diagrams* which show the interaction of foam facets with a chosen facet (or union of facets) in a foam, see Figure 4.
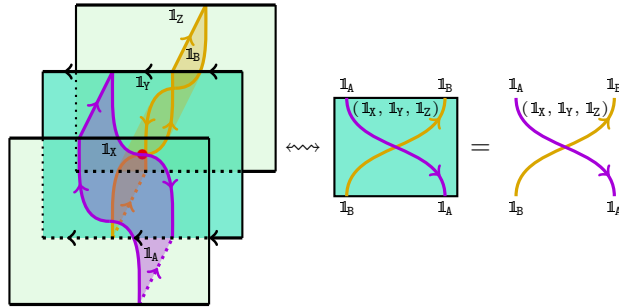
FIGURE 4. A phase diagram of a foam.

Here we adopt the convention that the facets lying in the drawing surface all carry the standard orientation of $\mathbb{R}^2$. The facets in front of the drawing surface are colored purple and those behind golden (and later also: cyan). For readers familiar with the relationship between foams and categorified quantum groups (as developed in [33, 34, 30, 39]), we emphasize that the orientation conventions in phase diagrams are not identical to those used in the string diagrams of the skew Howe dual categorified quantum group.

The first equations in Lemma 2.31 are simply

(2.18)

The following phase diagrams represent associativity and MP relations on foams, which hold in $\mathbb{S}\mathbf{Foam}$ by Proposition 2.19:

(2.19)

The relations obtained be reversing the orientation on all seams in (2.19) also hold. Similarly, the pitchfork moves hold for all possible orientations on seams in $\mathbb{S}\mathbf{Foam}$, see [39, Relations (3.28) and (3.29)] (imported via Proposition 2.19):

(2.20)

We will use several other versions of pitchfork relations, e.g.:

(2.21)   (2.22)

The relations of type (2.21) hold in $\mathbb{S}\mathbf{Foam}$ and can be deduced from (2.20) via (2.19). The relations of type (2.22) hold in $\mathbf{\Sigma Foam}$ and are obtained via (2.18).   ▲

Lemma 2.33. With $\mathtt{X} \subset \mathtt{A}$, the following phase diagram relations hold in $\mathbf{\Sigma Foam}$:

$$(2.23) \qquad = \frac{r(\mathtt{X},\mathtt{B})}{r(\mathtt{A} \setminus \mathtt{X}, \mathtt{X})} \quad , \qquad = \frac{r(\mathtt{B},\mathtt{X})}{r(\mathtt{X}, \mathtt{A} \setminus \mathtt{X})}$$

$$(2.24) \qquad = r(\mathtt{B},\mathtt{A}) \qquad , \qquad = r(\mathtt{B},\mathtt{A})$$

$$(2.25) \qquad = \frac{r(\mathtt{B},\mathtt{X})}{r(\mathtt{X}, \mathtt{A} \setminus \mathtt{X})} \qquad , \qquad = \frac{r(\mathtt{X},\mathtt{B})}{r(\mathtt{A} \setminus \mathtt{X}, \mathtt{X})}$$ □

Proof. Relation (2.23) is the shorthand notation for

$$= \frac{r(\mathtt{X},\mathtt{B})}{r(\mathtt{A} \setminus \mathtt{X}, \mathtt{X})}$$

which can be checked by detaching the annulus from the rear facet via (2.11) and collapsing the resulting blister in the front facet via (2.31). The relations in (2.24) and (2.25) follow analogously from the relations in Lemma 2.31 and MP relations.   ■

Note that planar isotopies of phase diagrams relative to their boundary correspond to isotopies of foams. Thus, relations obtained by isotoping any of the above relations continue to hold.

3. Equivariant, colored link homology via foams and its specializations

3.1. **Colored link homology.**
Given an additive, $\mathrm{Sym}(\mathbb{S})$-linear canopolis $\mathcal{C}$, we obtain from it an additive, $\mathrm{Sym}(\mathbb{S})$-linear canopolis of (bounded) complexes $\mathbf{Kom}(\mathcal{C})$ and chain maps between them. On chain complexes, the planar algebra operation is defined to take the planar composites of all chain groups, and the structure of differentials between them is modeled on the tensor product of chain complexes. More precisely, we require the inputs of all planar algebra operations to be ordered, which determines the order in which the formal tensor product is taken and thus, the *Koszul signs* in the differentials of the resulting tensor product complex.

Convention 3.1. The tensor product of two complexes (A^*, d_A) and (B^*, d_B) is defined to be:

$$(A \otimes B)^* = \bigoplus_{a+b=*} A^a \otimes B^b, \quad d_{(A \otimes B)^*} = \sum_{a+b=*} (-1)^b d_{A^a} \otimes \mathrm{id}_{B^b} + \mathrm{id}_{A^a} \otimes d_{B^b}$$

The reordering isomorphism $A \otimes B \cong B \otimes A$ is defined to act as $(-1)^{ab}$ times the swap map $A^a \otimes B^b \to B^b \otimes A^a$. Note that in the setting of a canopolis of chain complexes, where the swap map is the identity, the reordering isomorphisms act as the identity, except on terms of doubly-odd homological degree. This convention agrees with [12, Appendix A.6.1].   ▲

Since null-homotopic chain maps form an ideal with respect to planar algebra operations, it also makes sense to consider the homotopy canopolis of (bounded) complexes $\mathbf{K}(\mathcal{C})$ with morphisms given by chain maps up to homotopy. Forgetting the additional categorical structure in $\mathbf{Kom}(\mathcal{C})$ or $\mathbf{K}(\mathcal{C})$, we can also view both as planar algebras. A detailed discussion of these constructions is given in e.g. [2, Sections 3 and 4.1]. All these notions extend to the graded setup as well.

Convention 3.2. All links and tangles, as well as their diagrams, are assumed to be labeled (or *colored*) and oriented. Recall that two such tangle diagrams represent the same tangle if and only if the diagrams can be obtained from each other via a finite number of planar isotopies and Reidemeister moves as in Figure 10, i.e. the ones displayed therein as well as their orientation and crossing variations.   ▲

We consider the planar algebra of tangle diagrams $\mathbf{TD}$, which is generated by single strands, positive and negative crossings, as in Figure 5.
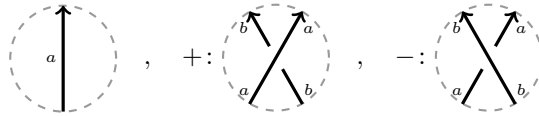
FIGURE 5. Generators of $\mathbf{TD}$.

Definition 3.3. Consider the map of planar algebras

(3.1) $[\![\cdot]\!] : \mathbf{TD} \to \mathbf{Kom}(\mathbb{S}\mathbf{Foam}^*),$

which is defined on generating tangle diagrams from Figure 5 as follows.

- It maps the a-labeled strand to the corresponding web, regarded as a complex concentrated in homological degree zero.
- It maps positive crossings with an overstrand labeled a and understrand labeled b with $a \geq b$ to:

(3.2)

$$\left[\!\!\left[\;\raisebox{-0.5em}{$\times$}\;\right]\!\!\right] \overset{a \geq b}{=} q^{-x} \xrightarrow{d_0^+} q^{1-x} \xrightarrow{d_1^+} \cdots$$

$$\cdots \xrightarrow{d_{b-2}^+} q^{b-1-x} \xrightarrow{d_{b-1}^+} q^{b-x}$$

Again, powers of q denote shifts in the q-degree, $x = b(N - b)$ and the underlined term is in homological degree zero. The differentials are given by the foams in Figure 6.

- A positive crossing with labels $b \geq a$ is mapped to the complex obtained from the one in (3.2) by reflecting webs in a vertical axis (and foams in a corresponding plane) and swapping labels a and b.
- The complexes for the negative crossings are obtained from the positive crossing complexes by inverting the q-degrees and the homological degrees, and reflecting the differential foams in a horizontal plane. ▲

$$d_k^+ =$$
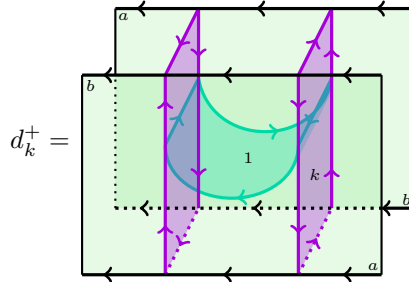
FIGURE 6. The differentials d_k^+. (The other differentials are similar.)

Example 3.4. In case $a = b = 1$ the complexes assigned to positive and negative crossings are of length two with differentials given by zip and unzip foams as in (2.5). ▲

Theorem 3.5. If T_D and T_D' are two tangle diagrams representing the same colored, oriented tangle, then $[\![T_D]\!] \cong [\![T_D']\!]$ holds in $\mathbf{K}(\mathbb{S}\mathbf{Foam})$. That is, $[\![\cdot]\!]$ is an invariant of colored, oriented tangles. □

Proof. Any reordering of the crossings in a tangle diagram induces an isomorphism between the respective invariants; so we disregard the ordering for the purpose of the following proof. By virtue of the planar algebraic construction, it suffices to show that the chain complexes associated to the tangles on both sides of each Reidemeister move are chain homotopy equivalent.

This result has already been proved in a variety of different categorifications of the MOY calculus, so we refer to the literature and only comment on the slight variations that we need.

The proof closest to our endeavour as regards generality has been given by Wu in [49, Proof of Theorem 1.1] in the context of his equivariant, colored link homology constructed via matrix factorizations. A proof purely in the language of webs and foams (although non-equivariant and with slightly different foam relations) has been first given by Mackaay–Stošić–Vaz [35, Section 7] for uncolored tangles. Queffelec–Rose [39, Section 4.3] have provided proofs for the Reidemeister moves that we will call (R2+) and (R3+) (see Section 3.3) for all colors. They have also described the behaviour of the invariant under *fork slides* and *fork twisting*, see [39, Proofs of Theorem 4.7 and Proposition 4.10]. These results immediately generalize to the equivariant setup with ground ring Sym($\mathbb{S}$) in $\mathbb{S}$**Foam** and—following Wu's strategy [49]—guarantee that the Reidemeister moves of type (R1), (R2–) and (R3–) hold for all colors if they hold in the uncolored case. The latter is easily checked by hand, e.g. analogous to the proof in [35, Section 7]. ∎

Remark 3.6. (Integrality.) Theorem 3.5 and its proof outlined above hold over $\mathbb{Z}$. In particular, the Reidemeister homotopy equivalences provided by Mackaay–Stošić–Vaz [35, Section 7] are manifestly integral. In the colored case, the Reidemeister homotopy equivalences used by Queffelec–Rose as well as their fork slides and fork twists are also integral, see [39, Proposition 4.10]. ▲

Definition 3.7. Let L_D be a colored, oriented link diagram. Then the equivariant, colored Khovanov–Rozansky homology of L_D is the bigraded, finite-rank Sym($\mathbb{S}$)-module defined as

$$\mathrm{KhR}^{\mathbb{S}}(L_D) = H_*(\mathcal{F}(\llbracket L_D \rrbracket)),$$

where $\mathcal{F}$ denotes the TQFT from Section 2.3.2. ▲

By Theorem 3.5, $\mathrm{KhR}^{\mathbb{S}}$ is invariant under Reidemeister moves and planar isotopies up to explicit isomorphisms.

If one sets the variables in the alphabet $\mathbb{S}$ equal to zero before applying an analog of the TQFT $\mathcal{F}$ in Definition 3.7, one obtains the (non-equivariant) bigraded, colored, Khovanov–Rozansky link homologies of Wu [48] and Yonezawa [50], see [42, Proposition 4.2] and [39, Theorem 4.11]. In the uncolored case, these agree with the original Khovanov–Rozansky link homologies [25].

More generally, the alphabet $\mathbb{S}$ can be specialized to any N-element multiset Σ of complex numbers, and one obtains deformed Khovanov–Rozansky link homologies KhR^{Σ}, see [49, 43]. In the next section, we will explain this in detail for $\Sigma = \Sigma$.

Remark 3.8. We have chosen a grading convention which results in a tangle invariant that respects the Reidemeister 1 move. Another natural grading convention leads to shifts under the Reidemeister 1 move, but has the advantage of allowing invariance under fork slide moves. We will not pursue this further in this paper. ▲

Remark 3.9. For the purpose of proving Theorem 3.5 it is not necessary to specify a particular pair of inverse chain homotopy equivalences for each Reidemeister move. Indeed, any such pair can be rescaled by a pair of inverse units in $\mathbb{C}$. However, for the purpose of defining chain maps associated to link cobordisms and for the proof of functoriality, such a specification is necessary. Arguments as in Section 4.2 imply that

the ambiguity is limited to rescaling by a unit in $\mathbb{C}$, and we will choose a particular scaling in Section 3.3. ▲

3.2. **Generic deformations and Karoubi envelope technology.** As before, let $\Sigma = \{\lambda_1, \ldots, \lambda_N\}$ be a set of N pairwise different complex numbers.

Lemma 3.10. ([43, Lemma 23].) In $\Sigma\textbf{Foam}$, the algebra of decorations on the identity foam on a web W is the direct sum of one-dimensional summands. The corresponding idempotents are given by colorings of all facets by idempotents as in Lemma 2.27, which are admissible in the sense of Lemma 2.28, i.e. the associated subsets of Σ add up around every singular seam. ∎

Recall that the Karoubi envelope $\textbf{Kar}(\mathcal{C})$ of a category $\mathcal{C}$ has as object pairs (O, e), where O is an object of $\mathcal{C}$ and $e\colon O \to O$ is an idempotent. The morphisms from (O, e) to (O', e') are morphisms of $\mathcal{C}$ compatible with the idempotents, i.e. triples (e, f, e') with $f\colon O \to O'$ such that $f \circ e = e' \circ f$ holds in $\mathcal{C}$. In case $\mathcal{C}$ is additive, one can split idempotents, i.e. by writing $O = (O, \text{id})$ and $\text{im}(e) = (O, e)$, we get

$$O \cong \text{im}(e) \oplus \text{im}(\text{id} - e) \quad (\text{in } \textbf{Kar}(\mathcal{C})).$$

We will use a full subcategory of $\textbf{Kar}(\Sigma\textbf{Foam})$ which contains all idempotents identified in Lemma 3.10.

Definition 3.11. Let $\Sigma\overline{\textbf{Foam}}$ denote the full additive, $\text{Sym}(\mathbb{S})$-linear subcategory of $\textbf{Kar}(\Sigma\textbf{Foam})$ containing all objects of the form $(W, c(W)\text{id}_W)$ as well as their q-degree shifts. Here W is a web and $c(W)\text{id}_W$ is an admissibly idempotent-colored identity foam on W as in Lemma 3.10. ▲

We shall think of the objects $(W, c(W)\text{id}_W)$ as idempotent-colored webs. $\Sigma\textbf{Foam}$ embeds as a full subcategory of $\Sigma\overline{\textbf{Foam}}$ since the identity foam on every web can be split into the sum of its idempotent-colorings. Correspondingly, uncolored webs can be split into direct sums of idempotent-colored webs. For example:

Here the direct sum runs over all a-element subsets $\texttt{A}$ of Σ. Another example is:

Note that the idempotent on the edge of the biggest label is determined by the other two due to the admissibility condition from Lemma 2.28.

We will denote by $[\![\cdot]\!]^\Sigma\colon \textbf{TD} \to \textbf{K}(\Sigma\textbf{Foam}) \subset \textbf{K}(\Sigma\overline{\textbf{Foam}}N)$ the Σ-specialization of $[\![\cdot]\!]$, obtained via post composition with sp^Σ from Section 2.5. From Theorem 3.5 we immediately obtain the following specialization:

Theorem 3.12. If T_D and T'_D are two tangle diagrams representing the same colored, oriented tangle, then $[\![T_D]\!]^\Sigma \cong [\![T'_D]\!]^\Sigma$ holds in $\textbf{K}(\Sigma\textbf{Foam})$. That is, $[\![\cdot]\!]^\Sigma$ is an invariant of colored, oriented tangles. □

The next lemma provides a decomposition of the complexes associated to crossings, which dramatically simplifies the computation of Σ-deformed link invariants. By convention, we indicate the homological degree using powers of t.

Lemma 3.13. The complex associated to a link in $\mathbf{K}(\Sigma\overline{\mathbf{Foam}})$ is isomorphic to a complex with trivial differentials, e.g. for $a \geq b$ we have locally:

$$(3.3) \qquad \left[\!\!\left[\begin{matrix} b \nearrow\!\!\!\nwarrow a \\ a \qquad b \end{matrix}\right]\!\!\right]^{\Sigma} \cong \bigoplus_{\mathtt{A},\mathtt{B}\subset\Sigma} \begin{matrix} \mathtt{B} \qquad \mathtt{A} \\ \diagdown\!\!\!\diagup \\ \mathtt{A} \qquad \mathtt{B} \end{matrix} \cong \bigoplus_{k=0,\ldots,b} \bigoplus_{\substack{\mathtt{A},\mathtt{B}\subset\Sigma, \\ |\mathtt{B}\backslash\mathtt{A}|=k}} t^k \quad \begin{matrix} \mathtt{B} \quad \mathtt{A} \\ {\scriptstyle\mathtt{AB}} \\ {\scriptstyle\mathtt{BA}} \\ \mathtt{A} \quad \mathtt{B} \end{matrix} \qquad\qquad \square$$

Here and in the following, we display a tangle diagram T_D with strands colored by idempotents as a shorthand notation for the corresponding idempotent-colored subcomplex of $[\![T_D]\!]^{\Sigma}$ in $\mathbf{K}(\Sigma\overline{\mathbf{Foam}})$. We also write $\mathtt{XY} = \mathtt{X} \setminus \mathtt{Y}$ for any two subsets $\mathtt{X}, \mathtt{Y} \subset \Sigma$. If a web edge is colored with $\mathtt{XY} = \emptyset$, then it is to be deleted from the diagram. The complexes associated to other crossings split analogously, with negative crossings receiving negative shifts in homological degree.

Proof. This is a special case of [43, Lemma 60]. ∎

In the case of $\Sigma = \{1, -1\}$ and $a = b = 1$, the decomposition (3.3) precisely recovers Blanchet's decomposition in [4, Figure 17].

3.3. **Simple resolutions and Reidemeister foams.** In this section we study the complexes associated to link diagrams in the Σ-deformation and the homotopy equivalences between them, which are induced by Reidemeister moves. This will also lead us to determine a particular scaling for the Reidemeister homotopy equivalences in $\mathbf{K}(\mathbb{S}\mathbf{Foam})$ that is necessary for the functoriality proof in Section 4.

As a first step, we apply Lemma 3.13 to all crossings in the link diagrams appearing in Reidemeister moves, and we immediately obtain:

Lemma 3.14. The following isomorphisms hold in $\mathbf{K}(\Sigma\overline{\mathbf{Foam}})$.

The Σ-deformed complexes associated to link diagrams appearing in other versions of Reidemeister moves have analogous simplifications. ∎

Lemma 3.15. Under the direct sum decompositions of complexes from Lemma 3.14, the homotopy equivalences associated to Reidemeister moves are given by diagonal matrices whose non-zero entries are invertible, idempotent-colored foams in $\Sigma\mathbf{Foam}$. The analogous result also holds for all possible colorings and orientations of Reidemeister moves, which do not appear in Lemma 3.14. $\square$

Proof. This follows from the facts that $\llbracket \cdot \rrbracket^\Sigma$ is a tangle invariant in $\mathbf{K}(\Sigma\overline{\mathbf{Foam}})$ by Theorem 3.12, and that any non-zero foam between colored webs preserves the idempotent-colors on the boundary edges of such webs. ∎

For the following, we choose (once and for all) an ordering of $\Sigma = \{\lambda_1, \dots \lambda_N\}$.

Definition 3.16. Our favourite idempotent-coloring of a tangle diagram T_D is given by coloring every a-labeled strand with the idempotent $\mathbb{1}_\mathtt{A}$ for $\mathtt{A} = \{\lambda_1, \dots, \lambda_a\} \subset \Sigma$. Lemma 3.13 implies that the subcomplex of $\llbracket T_D \rrbracket^\Sigma$ corresponding to this favourite idempotent-coloring simplifies to a single colored web of minimal combinatorial complexity, which we will call the *simple resolution* of T_D. ▲

Example 3.17. The simple resolutions of the tangle diagrams from Lemma 3.14 are obtained as follows:
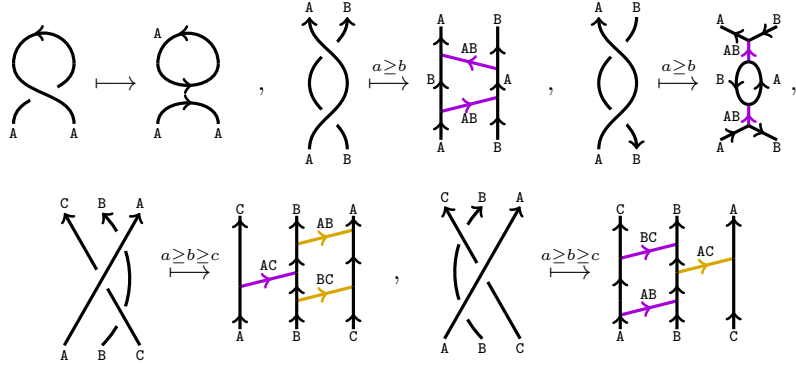
Here and in the following there are no homological degree shifts. Link diagrams which appear in other oriented versions of Reidemeister moves have similar simple resolutions. We will discuss this variety in more detail below. ▲

Lemma 3.18. The Reidemeister 1 and 2 homotopy equivalences in $\mathbf{K}(\Sigma\overline{\mathbf{Foam}})$ are realized on simple resolutions by complex multiples of the foams in Figure 7.

(R1) If a Reidemeister 1 move in a strand of label a increases the writhe of the link diagram, then the corresponding foams between simple resolutions has to be rescaled by $r(\mathtt{A})$. For example:
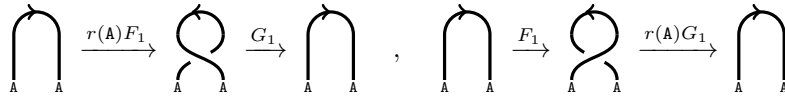
(R2+) For Reidemeister 2 moves between strands of labels a, b with parallel orientation, the foams F_2^+ and G_2^+ are normalized by a sign $\epsilon = (-1)^{\min(a,b)(a-b)}$ depending on which strand is pushed over. For example:
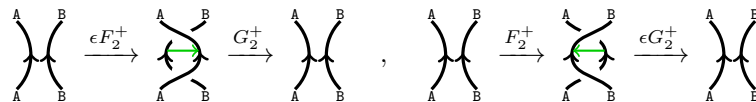
(R2–) For Reidemeister 2 moves between strands of labels a, b and opposite orienta-
tions, the foams F_2^- and G_2^- are also normalized by ϵ as follows:
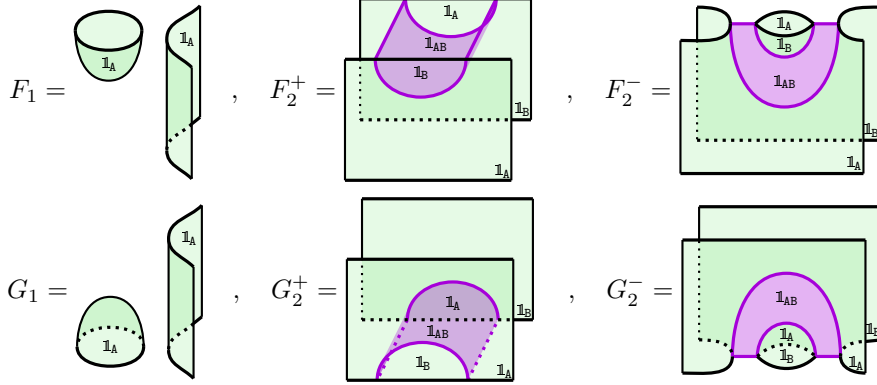
FIGURE 7. The (R1), (R2+) and (R2–) foams.

Proof. We first check the case of the Reidemeister 2 moves. Using Remark 2.15 and working in $\mathbf{K}(\mathbb{S}\mathbf{Foam})$, it is easy to see that the shown foams $F_2^{\pm}$ and $G_2^{\pm}$ (without their idempotent decoration) are uniquely determined up to a complex scalar by their degrees. This scalar is non-zero since these foams become invertible in $\Sigma\mathbf{Foam}$. It follows that F_2^+ and G_2^+ are mutually inverse up to a scalar ϵ, which is determined by Relation (2.15). This already holds in $\mathbb{S}\mathbf{Foam}$. On the contrary, F_2^- and G_2^- only become mutually inverse up to the same sign ϵ when considered in $\Sigma\mathbf{Foam}$ and decorated by idempotents as shown. This follows from the relations in Lemma 2.33. Now we can rescale the Reidemeister 2 homotopy equivalences in $\mathbb{S}\mathbf{Foam}$ to obtain units as in the statement of the lemma.

Regarding Reidemeister 1 moves, degree considerations in $\mathbb{S}\mathbf{Foam}$ using Remark 2.15 imply that the relevant foams are uniquely determined (up to a non-zero complex scalar) in the cases where we claim that no extra scalar appears. In the other cases, the foams carry a decoration and are determined (up to a unit) by the requirement to be a component of a chain map. More specifically, the decoration is the result of a neck-cut (2.9) and the scalar $r(\mathtt{A})$ results from specializing it (2.17). It follows that these decorated foams give mutual inverses in $\Sigma\mathbf{Foam}$, and so we choose to scale the Reidemeister 1 homotopy equivalences in $\mathbb{S}\mathbf{Foam}$ accordingly. ∎

Next, we describe the chain homotopy equivalences induced by Reidemeister 3 moves of type (R3+), whose local model involves tangles with a cyclic sequence of boundary orientations given by three outward pointing arcs followed by three inward pointing arcs, see e.g. (3.4). The remaining Reidemeister 3 moves, of type (R3–), have a boundary orientation sequence alternating between inward and outward pointing and will be dealt with at the end of this section.

Lemma 3.19. The homotopy equivalences induced by (R3+) moves are realized on simple resolutions by foams F_3^+ and G_3^+

(3.4)

which can be represented by phase diagrams with at most two trivalent vertices. See Figure 7 for illustrations of these foams in the case $a \geq b \geq c$. □
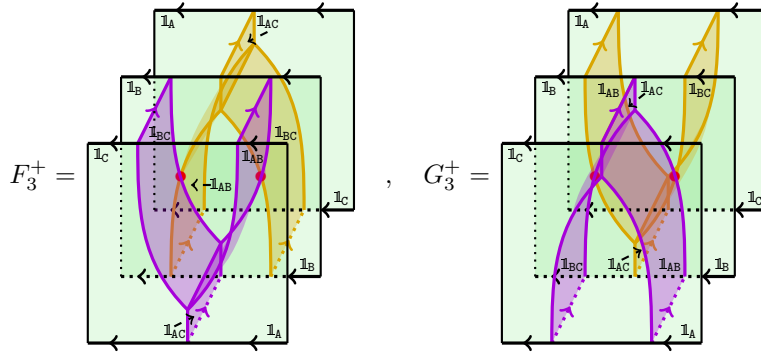
FIGURE 8. Examples of (R3+) foams.

Proof. As in the proof of Lemma 3.18, we deduce that Reidemeister 3 homotopy equivalences restrict to invertible, idempotent-colored foams on simple resolutions. Degree considerations in $\mathbb{S}\mathbf{Foam}$ determine these (up to a unit) to be foams that admit phase diagrams with at most two trivalent vertices. Note that they are the foams of lowest combinatorial complexity between these simple resolutions. Below we display phase diagrams for three labeling patterns and check that they represent mutually inverse foams in $\Sigma\mathbf{Foam}$. As before, this determines our preferred scaling of the Reidemeister 3 homotopy equivalences in $\mathbb{S}\mathbf{Foam}$.

For $a \geq b \geq c$, the composition $G_3^+ \circ F_3^+$ simplifies to the identity foam as follows:

Here we have applied (2.24) and (2.18). In the case $a \geq c \geq b$ the foam $G_3^+ \circ F_3^+$ simplifies as:

Here we used (2.19), (2.24), (2.23) and (2.25). In the similar case $b \geq a \geq c$ we get:

The other compositions $F_3^+ \circ G_3^+$ and all other cases can be checked to produce identity foams in a completely analogous way. Thus, we have shown that the (R3+) foams F_3^+ and G_3^+ are mutually inverse foams, which proves the statement. ∎

For Reidemeister 3 moves with alternating boundary orientations, i.e. type (R3–), we use the following composite of (R2–), (R2+) and (R3+):

$$(3.5) \qquad \text{}$$

This is also to be interpreted as a template for variations of the (R3–) moves with different crossing types than the one shown. In all cases, the active strand (the one participating in all (R2) moves) is chosen to be the first strand encountered on the boundary when proceeding in the counterclockwise direction, starting from the boundary of the top strand. This is indicated by arrows in (3.5). We denote the induced composite foams on simple resolutions by F_3^- and G_3^-:

Example 3.20. In the case $a \geq b \geq c$, the foams F_3^- and G_3^- are given by the following compositions reading left-to-right and right-to-left respectively:

$$(3.6) \qquad \text{}$$

Here ε and τ are signs coming from our scaling conventions. ▲

As for the other Reidemeister moves, the foams F_3^- and G_3^-, which are defined on simple resolutions in $\Sigma\mathbf{Foam}$, determine a particular scaling of the (R3–) homotopy equivalences in $\mathbb{S}\mathbf{Foam}$ that we henceforth adopt.

Example 3.21. In the case where all labels on strands are equal, the simple resolutions of the tangle diagrams appearing in Reidemeister moves and the foams between them are especially simple: (R2+) and (R3+) moves take the form of identity foams between identity webs, and (R2–) are realized by cup- and cap-saddles. In the (R3–) move from (3.6), the purple edges disappear and the resulting foam is a *monkey saddle* as in [2, Figure 9]. ▲

Above, we have determined a particular scaling for the Reidemeister move homotopy equivalences in $\mathbf{K}(\mathbb{S}\mathbf{Foam})$. Even though this process depends on the choice of a particular specialization Σ, the result is quite rigid.

Lemma 3.22. (Integrality.) The rescaled Reidemeister move homotopy equivalences are integral. □

Proof. Consider a particular Reidemeister move and denote by f and g the mutually inverse rescaled homotopy equivalences, which satisfy

$$(3.7) \qquad \mathrm{id} - f \circ g = d \circ h + h \circ d,$$

where d is the differential in the domain of g, h is a homotopy and all of these morphisms are built from foams with coefficients in $\mathbb{C}$. By the integral version of Theorem 3.5, see Remark 3.6, there also exist mutually inverse integral homotopy equivalences f' and g' as well as an integral homotopy h' such that

$$(3.8) \qquad \mathrm{id} - f' \circ g' = d \circ h' + h' \circ d.$$

Above we have seen that the foams appearing in f and g on simple resolutions are already integral. This implies that f' and g' are integer multiples of f and g, respectively.

Let $z_1, z_2 \in \mathbb{Z}$ be such that $f' = z_1 f$ and $g' = z_2 g$. Substituting in (3.8) and subtracting from it a multiple of (3.7) gives

$$(1 - z_1 z_2)\mathrm{id} = d \circ (h' - z_1 z_2 h) + (h' - z_1 z_2 h) \circ d.$$

Since the domain of g is not a contractible chain complex, this implies $z_1 z_2 = 1$. Consequently, $z_1 = z_2 = \pm 1$ and so $f = \pm f'$ and $g = \pm g'$ are integral. ■

4. FUNCTORIALITY

4.1. **The canopolis of tangles and their cobordisms in 4-space.** In Section 3.1 we have encountered the planar algebra $\mathbf{TD}$ of colored, oriented tangles. Now we extend it to a canopolis.

Definition 4.1. Let $\mathbf{TD}$ be the canopolis determined by the following data.

- The objects are given by colored, oriented tangle diagrams in disks D with an ordering of the crossings. We regard such diagrams as actual colored, oriented tangles, embedded in $D \times [0, 1]$.
- The morphisms (besides crossing reordering isomorphisms) are 2-dimensional colored, oriented cobordisms between tangles, embedded in $D \times [0, 1] \times [0, 1]$, cylindrical in a neighborhood of the boundary, with matching boundary orientation on the top boundary and opposite one on the bottom, modulo isotopy relative to the boundary.

- The categorical composition is given by gluing cobordisms vertically.
- The planar algebra operation by gluing horizontally and concatenating orders of crossings. ▲

If a cobordism C between tangles is in generic position, then the horizontal slices $C_z = C \cap (D \times [0,1] \times \{z\})$ give tangle diagrams, except for at most finitely many $z \in [0,1]$. At such a critical point, the tangle diagram $C_{z-\epsilon}$ transforms into the tangle diagram $C_{z+\epsilon}$ by a Morse or a Reidemeister move, see Figure 9 for examples.
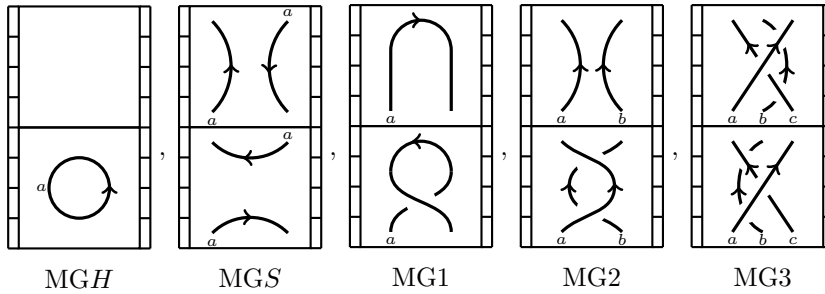

FIGURE 9. Examples of movies of generating cobordisms.

Between these critical values, the diagrams C_z differ only by planar isotopy. As a result, a cobordism C in generic position can be represented by a *movie* of tangle diagrams, whose consecutive frames show precisely the transformation of horizontal slices across a single critical value. Such movie presentations of cobordisms are not unique, but their ambiguity can be controlled, as we recall next. For this, we use a more rigid version of **TD** in which movie moves represent cobordisms uniquely:

Definition 4.2. Let $\mathbf{TD}^*$ be the canopolis with the same objects and canopolis operations as **TD**, but with morphisms given by cobordisms rigidly built from Morse and Reidemeister type cobordism generators, without allowing isotopy. ▲

By definition, morphisms in $\mathbf{TD}^*$ can be uniquely represented by movies of tangle diagrams, whose frames differ by a single Morse or Reidemeister type cobordism (together with a crossing reordering). The ambiguity of this presentation for cobordisms in **TD**, where we allow isotopies, is described in the following proposition.

Proposition 4.3. The rigidly built cobordisms in $\mathbf{TD}^*$, which are identified under the projection $\mathbf{TD}^* \to \mathbf{TD}$ are precisely those which can be related by finite sequences of the relations shown and explained in Figures 10, 11 and 12 as well as their variations obtained from changing orientations and the height of strands. □

These relations between cobordism movies are colored, oriented versions the *movie moves* as presented by Carter–Saito in [8, Chapter 2], but numbered as in [2, Section 8].

Proof. By forgetting colors and orientations, any isotopy of cobordisms in **TD** is, in particular, an isotopy of cobordisms as studied in [8, Chapter 2]. Hence, it can be written as a finite sequence of the movie moves therein. Remembering the coloring data and the orientation again, we see that the original isotopy in **TD** can be written as a finite sequence of the colored, oriented movie moves. ■
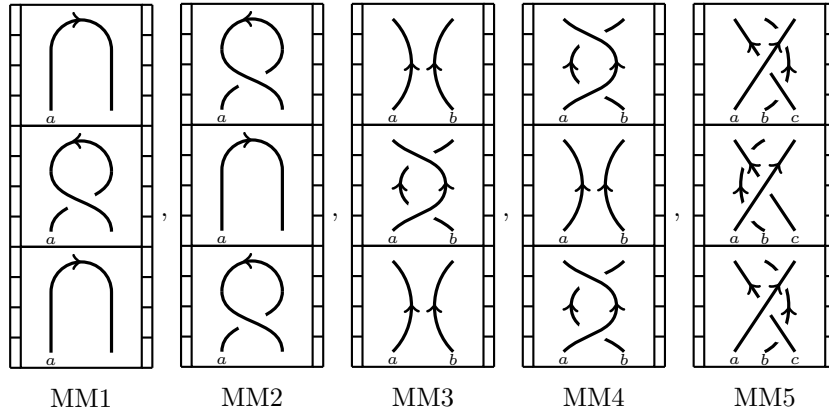
FIGURE 10. The reversible movie moves, which say that doing and undoing Reidemeister moves is equivalent to doing nothing.
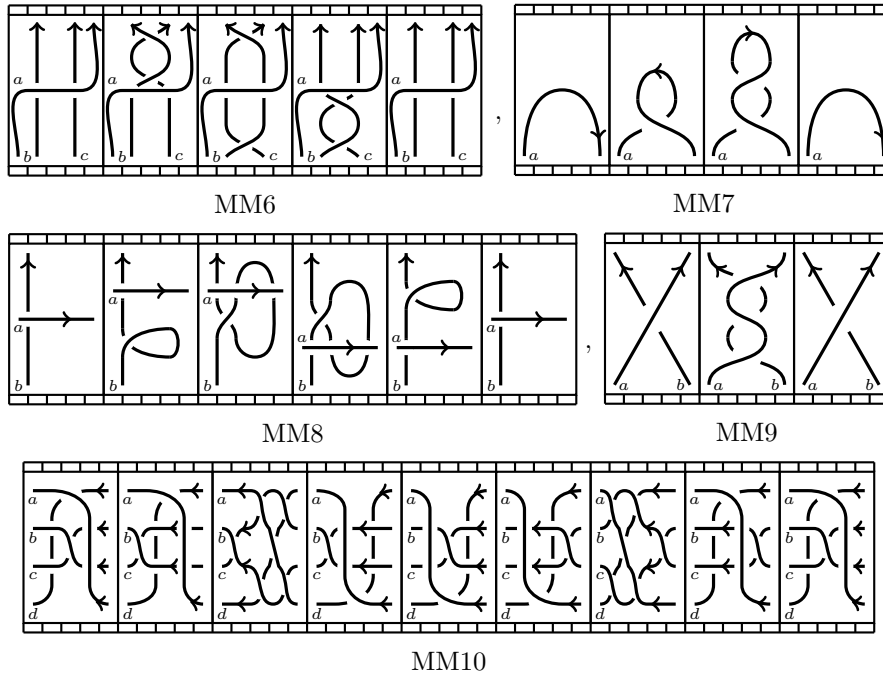

FIGURE 11. The reversible movie moves, which show movies equivalent to doing nothing if read left- or rightwards.

Now, we extend the definition of $[\![\cdot]\!]$ to a canopolis functor

$$[\![\cdot]\!] : \mathbf{TD}^* \to \mathbf{K}(\mathbb{S}\mathbf{Foam})$$

by assigning (homotopy classes of) chain maps to the generating cobordisms in Figure 9. To cups, saddles and caps, we associate the chain maps given by acting with the
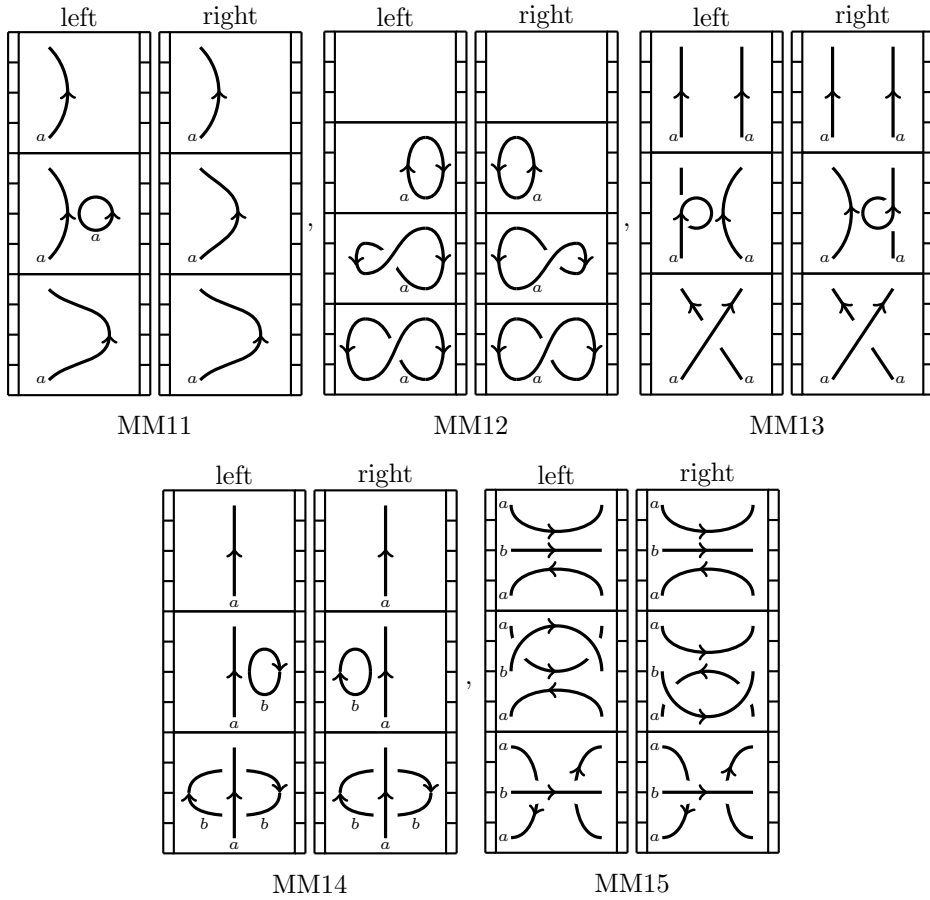
FIGURE 12. The non-reversible movie moves. The columns show equivalent movies when read down- or upwards.

corresponding foam from (2.4) on every chain group. To Reidemeister cobordisms we assign the corresponding Reidemeister homotopy equivalences with the scaling identified in Section 3.3. Finally, the crossing reordering isomorphisms are sent to the corresponding reordering isomorphisms in $\mathbf{K}(\mathbb{S}\mathbf{Foam})$.

Remark 4.4. By construction, $[\![\cdot]\!]$ assigns homotopy inverse chain maps to Reidemeister moves and their inverses. The chain maps assigned to movies from Figure 10 are thus, homotopic to the corresponding identity chain maps and we express this by saying that $[\![\cdot]\!]$ respects the movie moves MM1–MM5, see Theorem 3.5.   ▲

The main goal of this paper is to show that $[\![\cdot]\!]$ assigns equal (homotopy classes of) chain maps to cobordism movies which are related by one of the remaining movie moves MM6–MM15, and thus:

Theorem 4.5. (Functoriality.) The canopolis functor $[\![\cdot]\!] : \mathbf{TD}^* \to \mathbf{K}(\mathbb{S}\mathbf{Foam})$ factors through a functor

$$[\![\cdot]\!] : \mathbf{TD} \to \mathbf{K}(\mathbb{S}\mathbf{Foam}).$$ □

The proof of this theorem is contained in the following two sections. First we use an abstract argument to see that $\llbracket \cdot \rrbracket$ respects movie moves up to scalars in $\mathbb{C}$. Finally, in Section 4.3, we compute these scalars via the Σ-deformation and find them to be equal to one.

4.2. **Functoriality up to scalars.** We follow Bar-Natan's strategy [2, Section 8] to show that $\llbracket \cdot \rrbracket$ respects movie moves up to scalars in $\mathbb{C}$. The following Lemma contains the key idea of this strategy.

Lemma 4.6. Let T_D be a diagram of a tangle which is isotopic (without fixing boundary points) to a trivial tangle. Then the space of degree zero endomorphisms of $\llbracket T_D \rrbracket \in \mathbf{K}(\mathbb{S}\mathbf{Foam})$ is one-dimensional over $\mathbb{C}$. $\hspace{1em}\square$

Proof. Since planar composition with crossings on the boundary is an invertible operation, the problem reduces to the case where T_D is a trivial tangle diagram supported in homological degree zero, see [2, Lemmas 8.7, 8.8 and 8.9]. For such we have already observed in Remark 2.15 that the space of degree zero endomorphisms is one-dimensional. $\hspace{1em}\blacksquare$

Proposition 4.7. The movie moves hold up to scalars in $\mathbf{K}(\mathbb{S}\mathbf{Foam})$. $\hspace{1em}\square$

Proof. For the reversible movie movies from Figure 11, it follows immediately from Lemma 4.6 that the chain map associated to the complicated movie agrees up to a complex scalar with the identity chain map. Additionally, since it is a composition of homotopy equivalences, it is invertible, and thus, non-zero.

For the non-reversible movies from Figure 12 we first check that the morphism spaces between the initial and final frames of the movies are one-dimensional over $\mathbb{C}$ in the relevant degrees. For MM11 we have already seen this and MM13 is treated analogously after expanding the crossing into a chain complex. For the others movie moves, one can cut boring scenes from the movie during which only homotopy equivalences happen. It remains to analyze frames differing by Morse moves. The corresponding morphisms spaces have been identified to be one-dimensional in Remark 2.15. This shows that the chain maps associated to the two sides of such a movie move agree up to a scalar. $\hspace{1em}\blacksquare$

At this point, the non-reversible movie moves might hold only trivially, i.e. both sides might represent the zero chain map. However, in the next section we shall see that these maps are never zero.

Remark 4.8. (Integrality.) The proof of functoriality up to scalars over $\mathbb{Z}$ is completely analogous. Here we use that all morphism spaces are free $\mathrm{Sym}_{\mathbb{Z}}(\mathbb{S})$-modules, see Remark 3.6. $\hspace{1em}\blacktriangle$

4.3. **Computing the scalars.** It remains to compute the scalars by which the chain maps associated to the two sides of a movie move MM6–MM15 might differ. We check this on the Σ-deformations.

Lemma 4.9. If the movie moves hold non-trivially in $\mathbf{K}(\Sigma\overline{\mathbf{Foam}})$, then they hold non-trivially in $\mathbf{K}(\mathbb{S}\mathbf{Foam})$. $\hspace{1em}\square$

Proof. Since we already know that the movie moves hold in $\mathbf{K}(\mathbb{S}\mathbf{Foam})$ up to scalars in $\mathbb{C}$, these scalars can be computed after specializing to $\mathbf{K}(\Sigma\mathbf{Foam})$ and further embedding in $\mathbf{K}(\Sigma\overline{\mathbf{Foam}})$. The assumption guarantees that all these scalars are all equal to one. $\hspace{1em}\blacksquare$

Lemma 4.10. If the movie moves hold non-trivially on simple resolutions, then they hold non-trivially in $\mathbf{K}(\Sigma\overline{\mathbf{Foam}})$. $\qquad\square$

Proof. By specializing Proposition 4.7, we see that, up scalars in $\mathbb{C}$, the movie moves hold in $\mathbf{K}(\Sigma\overline{\mathbf{Foam}})$. Next, if two chain maps agree up to a scalar, this scalar can be computed by comparing the chain maps restricted to a subcomplex where one of them acts non-trivially. Here we choose the subcomplex in $\mathbf{K}(\Sigma\overline{\mathbf{Foam}})$ given by a simple resolution. $\qquad\blacksquare$

In the following, we shall compute the chain maps appearing in the movie moves MM6–MM15 when restricted to simple resolutions. We will find that the chain maps on both sides of each movie move agree and are non-zero. This will satisfy the assumption in Lemma 4.10 and consequently Lemma 4.9 and, thus, complete the proof of Theorem 4.5.

Remark 4.11. The simple resolutions of a tangle diagram are invariant under interchanging any number of positive and negative crossing (up to q-degree shifts which we ignore here). Moreover, thanks to Convention 3.1 and the fact that simple resolutions of crossings are supported in even homological degree (namely zero), we do not need to consider reordering isomorphisms, since they all act by the identity. Altogether, this allows us to reduce the number of different variants of movie moves which we need to check.

However, the maps associated to Reidemeister cobordisms are usually dependent on the relative sizes of the labels on strands as well as the height ordering of strands. In checking the movie moves, we shall display one such variant for each choice and comment on the others. $\qquad\blacktriangle$

Lemma 4.12. The movie move MM6 holds on simple resolutions. $\qquad\square$

Proof. MM6 has two essentially different versions depending on the relative orientation of the strands between which Reidemeister 2 moves happen. The first version involves two (R2+) and (R3+) moves. For $a \geq b \geq c$ it is given on simple resolutions as:
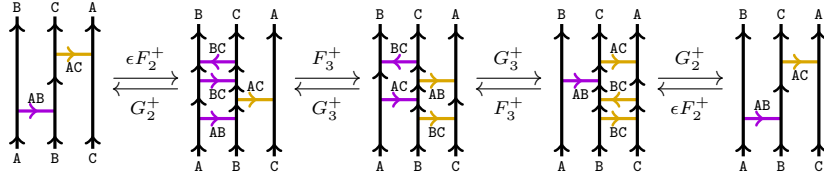
Here $\epsilon = (-1)^{c(b-c)}$. The composite foam for reading left-to-right is as follows.
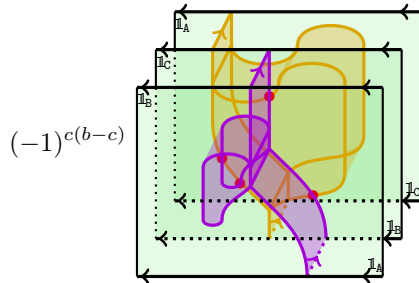
We compute that this foam is equal to the identity foam by simplifying its phase diagram using the relations obtained in Section 2.5.

$$(-1)^{c(b-c)} \quad \mathbb{1}_{\mathsf{AB}} \quad = (-1)^{c(b-c)} \quad \mathbb{1}_{\mathsf{BC}} \quad = \frac{(-1)^{c(b-c)}}{r(\mathsf{BC},\mathsf{AB})} \quad \mathbb{1}_{\mathsf{BC}} \quad = \mathbb{1}_{\mathsf{AB}} \quad \mathbb{1}_{\mathsf{BC}} \quad =$$

Here we have used (2.19), (2.24), (2.23) and (2.18). Since this movie move is composed out of homotopy equivalences, its inverse right-to-left read version also gives the identity on simple resolutions. The cases of relative orderings of colors differing from $a \geq b \geq c$ and, more generally, all other versions of MM6 which involve (R2+) moves are proved analogously.

The second version of the movie move MM6 not only involves two (R2–) moves, but also an (R3–) move, whose associated chain map we have defined as a composition of one (R3+) and several (R2±) chain maps. The composition of these maps can be read off as a the outer cycle of (R3+) and (R2±) chain maps in the following diagram, starting at the (marked) tangle diagram on the left.
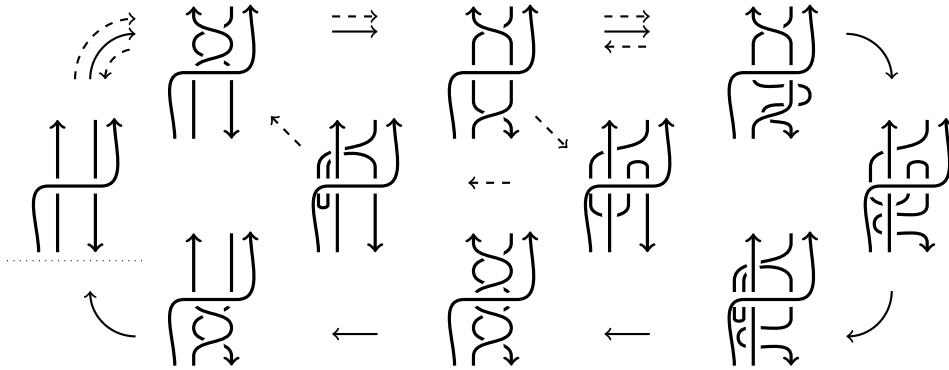
Our task is to see that this cycle is equivalent to the identity chain map on the complex associated to the left tangle diagram. First note that the final (R2–) move in the cycle far-commutes with the four moves preceding it. The resulting composition is indicated by dashed arrows, which now involve the middle tangle diagrams. Next, observe that the first and last step in the dashed cycle are inverse (R2–) moves. The detour through the tangle diagram on the left can thus, be cut from the dashed cycle. Similarly, there is another detour through the tangle diagram on the top right, which can be cut out by MM9 (which is proved independently in Lemma 4.15). It remains to confirm that there is no monodromy around the dashed rhombus. After omitting the top left crossing from the diagrams, which does not participate in these moves, we recognize the required check as a comparison of two ways of performing a (R3+) move.

The absence of monodromy can be checked on simple resolutions, e.g. for $a \geq b \geq c$:
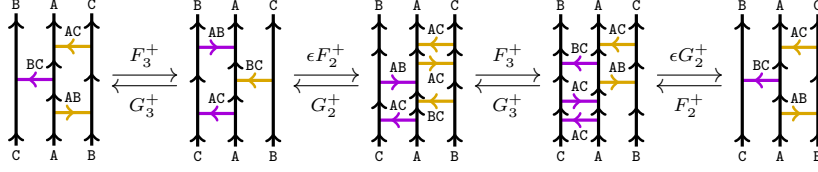
Again, $\epsilon = (-1)^{c(b-c)}$, and we have rotated the webs to have boundary orientations pointing upward. A routine calculation using phase diagrams now verifies that the composite from left-to-right (and vice versa) is the identity.

Note that all other variants of MM6 involving two (R2–) moves can be proven similarly using the short-cut strategy from above. Variants with a relative orderings of colors differing from $a \geq b \geq c$ can be treated analogously. ∎

Lemma 4.13. The movie move MM7 holds on simple resolutions. □

Proof. For the version displayed in Figure 11, we get the following behavior on simple resolutions:
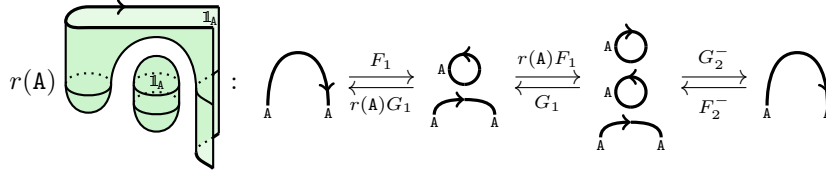
The foam displayed on the left gives the left-to-right composition of chain maps on simple resolutions. The idempotent-colored sphere cancels with the scalar $r(\mathtt{A})$ by (2.17). The remaining foam is isotopic to the identity. The other variants have analogous proofs. ∎

Lemma 4.14. The movie move MM8 holds on simple resolutions. □

Proof. The version of this movie move that is displayed in Figure 11 has the following behavior on simple resolutions if $a \geq b$:
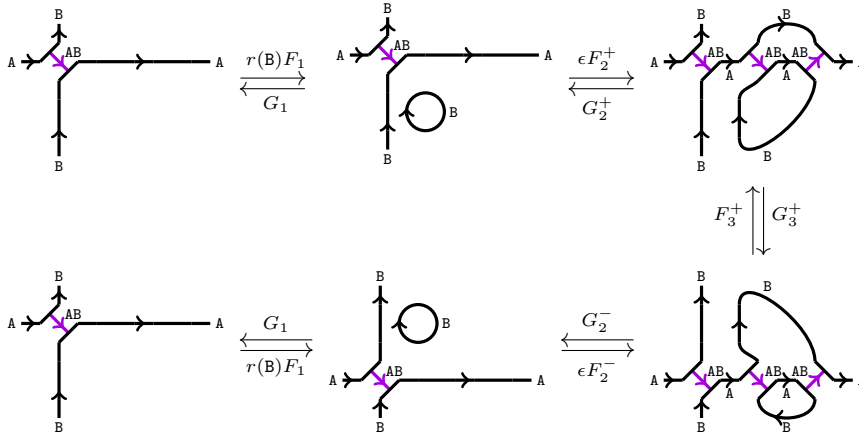
Here $\epsilon = (-1)^{b(a-b)}$. Note that, due to the involvement of only two different labels, the foams F_3^+ and G_3^+ are trivial. The composite, thus, takes the following form.
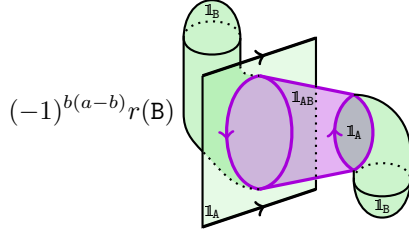

In this illustration we have omitted a trivial part to the foam. The sign $(-1)^{b(a-b)}$ and the scalar $r(\mathrm{B})$ precisely cancel with the scalars appearing in (2.15) and (2.17) when we delete the purple annulus and remove the resulting $\mathbb{1}_\mathrm{B}$-colored sphere on the right hand side of the diagram. The result is isotopic to an identity foam.

The reversed reading direction, the case $b \geq a$ and all other variations obtained by changing orientations or crossings are proved analogously. In each case, a foam of the above type (possibly with changed orientations and colorings) is simplified to give scalars as above. These precisely cancel with the normalizations of the Reidemeister foams since one always encounters a (R1) foam and its inverse, one essentially trivial (R3+) foam as well as (R2+) and (R2–) foams in inverse pairs. ∎

Lemma 4.15. The movie move MM9 holds on simple resolutions. □

Proof. This move has essentially two variants, which consist of either two (R2+) or (R2–) moves. For $a \geq b$ they take the following form on simple resolutions:
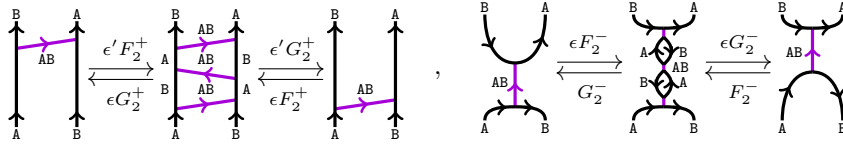
Here ϵ and ϵ' are the signs coming from the scaling of the Reidemeister foams, but which are irrelevant as they cancel in the composition. The composite foams are isotopic to identity foams, e.g. for the compositions from left to right we get:
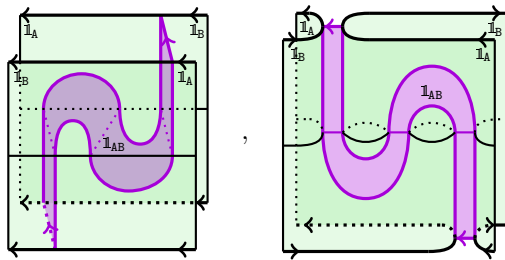

The case $a < b$ can be proven analogously. ∎

Lemma 4.16. The movie move MM10 holds on simple resolutions. □

Proof. This movie move exists in a large number of variants, all of which are equivalent modulo far-commutation and the already established MM6 by a beautiful argument of Clark–Morrison–Walker [12, Proof of MM10]. This directly extends to the colored

case and we only need to check the variant of MM10 displayed in Figure 11 for $a \geq b \geq c \geq d$. It is given on simple resolutions as the following composite starting at the top left diagram:
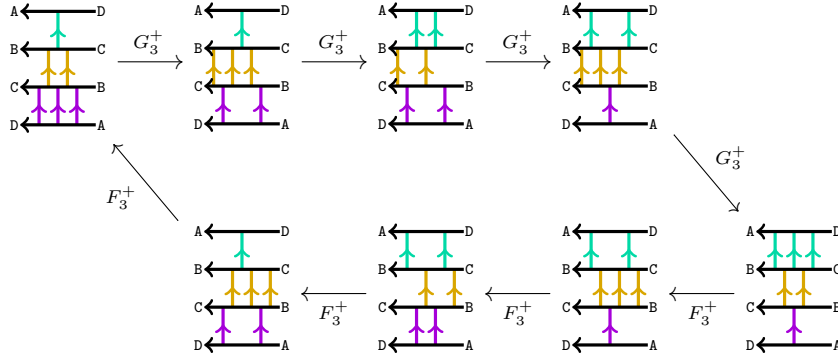
The composite of the first four maps G_3^+ is given by the following foam:

$$(4.1) \qquad$$
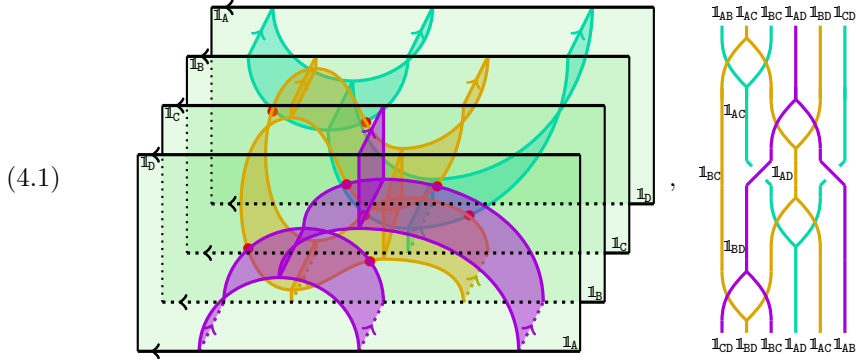
The composite of the remaining four maps F_3^+ is given by the foam obtained from the one above by reflecting in a line perpendicular to the green facets. The complete movie is thus represented by a phase diagram , which is symmetric in the origin of $\mathbb{R}^2$, the lower half of which is displayed in (4.1). It remains to show that this phase diagram represents the identity foam. As a first step, we focus on the interaction of purple and golden facets on the second green upright plane. This allows us to draw orientations on the phase diagram and the following simplification:

$$(4.2) \qquad$$
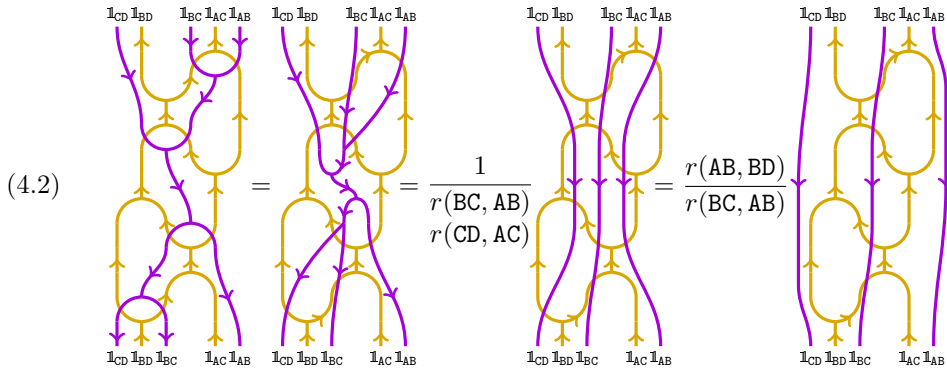
The outer two purple seams are completely separated from the rest of the diagram and will not be displayed in subsequent computations.

In the second step, we aim to simplify the golden facets of the foam. For this we observe that can locally apply relations of the form:

$$(4.3) \qquad \ldots = r(\mathtt{BC}, \mathtt{Y}) \ldots = r(\mathtt{BC}, \mathtt{Y}) \ldots = \ldots$$

Here $\mathtt{Y} = \mathtt{AB} \cup \mathtt{CD}$. After pushing the cyan facets outwards in a manner analogous to the first step in (4.2), we can perform the final sequence of simplifications. For this, we start with two applications of relations of type (4.3) (with parallel running purple and cyan strands in the middle):

$$\frac{r(\mathtt{AB},\mathtt{BD})}{r(\mathtt{BC},\mathtt{AB})} \ldots = \frac{r(\mathtt{AB},\mathtt{BD})}{r(\mathtt{BC},\mathtt{AB})} \ldots \frac{r(\mathtt{AB},\mathtt{CD})}{r(\mathtt{AB},\mathtt{BC})} r(\mathtt{CD},\mathtt{BC}) \ldots$$

$$\frac{1}{r(\mathtt{CD},\mathtt{BC})} r(\mathtt{AB},\mathtt{BC}) \ldots = \frac{r(\mathtt{CD},\mathtt{AB})}{r(\mathtt{BC},\mathtt{CD})} r(\mathtt{AB},\mathtt{BC}) \ldots = \frac{(-1)^{(a-b)(b-c)}}{r(\mathtt{CD},\mathtt{AB})} \ldots$$

In these steps have indicated the interaction of golden facets with purple and cyan ones, but we do not draw orientations.

The simplification use the phase diagram relations from Section 2.5, which also exhibit the last diagram as an identity foam in disguise. ∎

We skip MM11 as this just encodes an isotopy relation. For the remaining non-reversible movie moves, we denote the chain maps corresponding to cups, saddles and caps by M_0, M_1 and M_2.

Lemma 4.17. The movie move MM12 holds on simple resolutions. □

Proof. The movie on left-hand side in Figure 12 is given on simple resolutions by:

$$\emptyset \quad \underset{M_2}{\overset{M_0}{\rightleftarrows}} \quad \bigcirc_A \quad \underset{r(\mathtt{A})M_2}{\overset{M_0}{\rightleftarrows}} \quad \bigcirc_A \bigcirc_A$$

From the right-hand side we get:

$$\emptyset \quad \underset{M_2}{\overset{M_0}{\rightleftarrows}} \quad \bigcirc_A \quad \underset{r(\mathtt{A})M_2}{\overset{M_0}{\rightleftarrows}} \quad \bigcirc_A \bigcirc_A$$

These composites differ from the former ones only by isotopies.   ∎

Lemma 4.18. *The movie move MM13 holds on simple resolutions.*   □

Proof. Again, we compare the movies on the left- and right-hand sides in Figure 12 on simple resolutions:
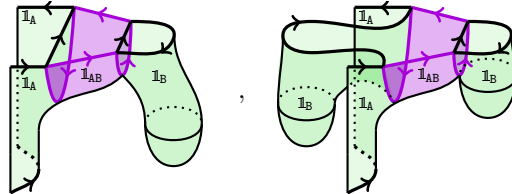

These foams differ only by isotopies.   ∎

Lemma 4.19. *The movie move MM14 holds on simple resolutions.*   □

Proof. Again, we compare the movies on the left- and right-hand sides in Figure 12 on simple resolutions for $a \geq b$:
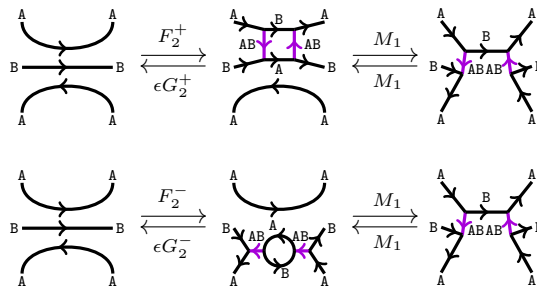

The scalars are identical and the foams are isotopic, e.g. reading left-to right gives:


The case $b \geq a$ and a second variant with different relative orientations is proved analogously.   ∎

Lemma 4.20. *The movie move MM15 holds on simple resolutions.*   □

Proof. In the left- and right-hand cases from Figure 12, the movie takes the following form on the simple resolutions for $a \geq b$:

As before, it remains to compare the composite foams since the scalars are the same. For reading left-to-right we get the following two isotopic foams:
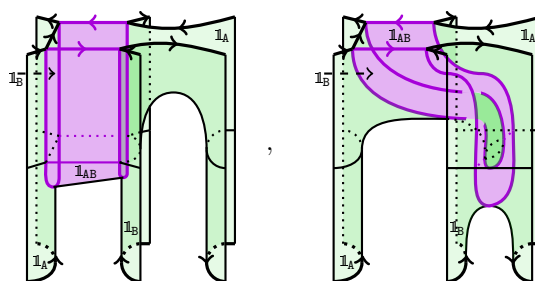
The other reading direction, the case $b \geq a$, as well as the variant obtained by switching orientations of the a-labeled strands work similar. ∎

Remark 4.21. (Integrality.) We know that also in the integral case, the chain maps on both sides of the movie moves differ by at most a scalar. That these scalars are all equal to one follows by extending scalars to $\mathbb{C}$, specializing via sp^Σ and using the results of this section. This is possible since the scaling for Reidemeister homotopy equivalences used here is integral by Lemma 3.22. ▲

References

[1] J.A. Baldwin, A.S. Levine, and S. Sarkar. Khovanov homology and knot Floer homology for pointed links. *J. Knot Theory Ramifications*, 26(2):1740004, 49, 2017. URL: https://arxiv.org/abs/1512.05422, doi:10.1142/S0218216517400041.

[2] D. Bar-Natan. Khovanov's homology for tangles and cobordisms. *Geom. Topol.*, 9:1443–1499, 2005. URL: http://arxiv.org/abs/math/0410495, doi:10.2140/gt.2005.9.1443.

[3] D. Bar-Natan and S. Morrison. The Karoubi envelope and Lee's degeneration of Khovanov homology. *Algebr. Geom. Topol.*, 6:1459–1469, 2006. URL: http://arxiv.org/abs/math/0606542, doi:10.2140/agt.2006.6.1459.

[4] C. Blanchet. An oriented model for Khovanov homology. *J. Knot Theory Ramifications*, 19(2):291–312, 2010. URL: http://arxiv.org/abs/1405.7246, doi:10.1142/S0218216510007863.

[5] C. Blanchet, N. Habegger, G. Masbaum, and P. Vogel. Topological quantum field theories derived from the Kauffman bracket. *Topology*, 34(4):883–927, 1995. doi:10.1016/0040-9383(94)00051-4.

[6] C.L. Caprau. $\mathfrak{sl}(2)$ tangle homology with a parameter and singular cobordisms. *Algebr. Geom. Topol.*, 8(2):729–756, 2008. URL: http://arxiv.org/abs/0707.3051, doi:10.2140/agt.2008.8.729.

[7] J.S. Carter. Reidemeister/Roseman-type moves to embedded foams in 4-dimensional space. In *New ideas in low dimensional topology*, volume 56 of *Ser. Knots Everything*, pages 1–30. World Sci. Publ., Hackensack, NJ, 2015. URL: https://arxiv.org/abs/1210.3608, doi:10.1142/9789814630627_0001.

[8] J.S. Carter and M. Saito. *Knotted surfaces and their diagrams*, volume 55 of *Mathematical Surveys and Monographs*. American Mathematical Society, Providence, RI, 1998.

[9] S. Cautis. Clasp technology to knot homology via the affine Grassmannian. *Math. Ann.*, 363(3-4):1053–1115, 2015. URL: https://arxiv.org/abs/1207.2074, doi:10.1007/s00208-015-1196-x.

[10] S. Cautis, J. Kamnitzer, and S. Morrison. Webs and quantum skew Howe duality. *Math. Ann.*, 360(1-2):351–390, 2014. URL: http://arxiv.org/abs/1210.6437, doi:10.1007/s00208-013-0984-4.

[11] D. Clark. Functoriality for the $\mathfrak{su}_3$ Khovanov homology. *Algebr. Geom. Topol.*, 9(2):625–690, 2009. URL: https://arxiv.org/abs/0806.0601, doi:10.2140/agt.2009.9.625.

[12] D. Clark, S. Morrison, and K. Walker. Fixing the functoriality of Khovanov homology. *Geom. Topol.*, 13(3):1499–1582, 2009. URL: http://arxiv.org/abs/math/0701339, doi:10.2140/gt.2009.13.1499.

[13] M. Ehrig, C. Stroppel, and D. Tubbenhauer. Generic $\mathfrak{gl}_2$-foams, web and arc algebras. URL: http://arxiv.org/abs/1601.08010.

[14] M. Ehrig, C. Stroppel, and D. Tubbenhauer. The Blanchet–Khovanov algebras. In *Categorification and Higher Representation Theory*, volume 683 of *Contemp. Math.*, pages 183–226. Amer. Math. Soc., Providence, RI, 2017. URL: http://arxiv.org/abs/1510.04884, doi:10.1090/conm/683.

[15] M. Ehrig, D. Tubbenhauer, and A. Wilbert. Singular TQFTs, foams and type D arc algebras. URL: http://arxiv.org/abs/1611.07444.

[16] W. Fulton. Equivariant cohomology in algebraic geometry. Eilenberg lectures, Columbia University, Spring 2007. Notes by D. Anderson. URL: https://people.math.osu.edu/anderson.2804/eilenberg/.

[17] B. Gornik. Note on Khovanov link cohomology. URL: http://arxiv.org/abs/math/0402266.

[18] M. Hedden and Y. Ni. Khovanov module and the detection of unlinks. *Geom. Topol.*, 17(5):3027–3076, 2013. URL: https://arxiv.org/abs/1204.0960, doi:10.2140/gt.2013.17.3027.

[19] M. Jacobsson. An invariant of link cobordisms from Khovanov homology. *Algebr. Geom. Topol.*, 4:1211–1251 (electronic), 2004. URL: http://arxiv.org/abs/math/0206303, doi:10.2140/agt.2004.4.1211.

[20] V.F.R. Jones. Planar algebras, I. URL: http://arxiv.org/abs/math/9909027.

[21] M. Khovanov. A categorification of the Jones polynomial. *Duke Math. J.*, 101(3):359–426, 2000. URL: http://arxiv.org/abs/math/9908171, doi:10.1215/S0012-7094-00-10131-7.

[22] M. Khovanov. Categorifications of the colored Jones polynomial. *J. Knot Theory Ramifications*, 14(1):111–130, 2005. URL: https://arxiv.org/abs/math/0302060, doi:10.1142/S0218216505003750.

[23] M. Khovanov. Link homology and Frobenius extensions. *Fund. Math.*, 190:179–190, 2006. URL: https://arxiv.org/abs/math/0411447, doi:10.4064/fm190-0-6.

[24] M. Khovanov. $\mathfrak{sl}(3)$ link homology. *Algebr. Geom. Topol.*, 4:1045–1081, 2004. URL: http://arxiv.org/abs/math/0304375, doi:10.2140/agt.2004.4.1045.

[25] M. Khovanov and L. Rozansky. Matrix factorizations and link homology. *Fund. Math.*, 199(1):1–91, 2008. URL: http://arxiv.org/abs/math/0401268, doi:10.4064/fm199-1-1.

[26] M. Khovanov and L. Rozansky. Topological Landau–Ginzburg models on the world-sheet foam. *Adv. Theor. Math. Phys.*, 11(2):233–259, 2007. URL: https://arxiv.org/abs/hep-th/0404189.

[27] D. Krasner. Equivariant $\mathfrak{sl}(n)$-link homology. *Algebr. Geom. Topol.*, 10(1):1–32, 2010. URL: https://arxiv.org/abs/0804.3751, doi:10.2140/agt.2010.10.1.

[28] G. Kuperberg. Spiders for rank 2 Lie algebras. *Comm. Math. Phys.*, 180(1):109–151, 1996. URL: http://arxiv.org/abs/q-alg/9712003.

[29] A. Lascoux. Notes on interpolation in one and several variables. URL: http://phalanstere.univ-mlv.fr/~al/pub_engl.html.

[30] A.D. Lauda, H. Queffelec, and D.E.V. Rose. Khovanov homology is a skew Howe 2-representation of categorified quantum $\mathfrak{sl}(m)$. *Algebr. Geom. Topol.*, 15(5):2517–2608, 2015. URL: http://arxiv.org/abs/1212.6076, doi:10.2140/agt.2015.15.2517.

[31] E.S. Lee. An endomorphism of the Khovanov invariant. *Adv. Math.*, 197(2):554–586, 2005. URL: http://arxiv.org/abs/math/0210213, doi:10.1016/j.aim.2004.10.015.

[32] I.G. Macdonald. *Symmetric functions and Hall polynomials*. Oxford Mathematical Monographs. The Clarendon Press, Oxford University Press, New York, second edition, 1995. With contributions by A. Zelevinsky, Oxford Science Publications.

[33] M. Mackaay. $\mathfrak{sl}(3)$-Foams and the Khovanov–Lauda categorification of quantum $\mathfrak{sl}(k)$. URL: https://arxiv.org/abs/0905.2059.

[34] M. Mackaay, W. Pan, and D. Tubbenhauer. The $\mathfrak{sl}_3$-web algebra. *Math. Z.*, 277(1-2):401–479, 2014. URL: http://arxiv.org/abs/1206.2118, doi:10.1007/s00209-013-1262-6.

[35] M. Mackaay, M. Stošić, and P. Vaz. $\mathfrak{sl}_N$-link homology ($N \geq 4$) using foams and the Kapustin–Li formula. *Geom. Topol.*, 13(2):1075–1128, 2009. URL: http://arxiv.org/abs/0708.2228, doi:10.2140/gt.2009.13.1075.

[36] M. Mackaay and P. Vaz. The universal $\mathfrak{sl}_3$-link homology. *Algebr. Geom. Topol.*, 7:1135–1169, 2007. URL: https://arxiv.org/abs/math/0603307, doi:10.2140/agt.2007.7.1135.

[37] M. Mackaay and B. Webster. Categorified skew Howe duality and comparison of knot homologies. URL: https://arxiv.org/abs/1502.06011.

[38] H. Murakami, T. Ohtsuki, and S. Yamada. Homfly polynomial via an invariant of colored plane graphs. *Enseign. Math. (2)*, 44(3-4):325–360, 1998.

[39] H. Queffelec and D.E.V. Rose. The $\mathfrak{sl}_n$ foam 2-category: a combinatorial formulation of Khovanov–Rozansky homology via categorical skew Howe duality. *Adv. Math.*, 302:1251–1339, 2016. URL: http://arxiv.org/abs/1405.5920, doi:10.1016/j.aim.2016.07.027.

[40] J. Rasmussen. Khovanov homology and the slice genus. *Invent. Math.*, 182(2):419–447, 2010. URL: http://arxiv.org/abs/math/0402131, doi:10.1007/s00222-010-0275-6.

[41] L.-H. Robert. Categorification of the colored $\mathfrak{sl}_3$-invariant. *J. Knot Theory Ramifications*, 25(7):1650038, 43, 2016. URL: https://arxiv.org/abs/1503.08451, doi:10.1142/S0218216516500383.

[42] L.-H. Robert and E. Wagner. A closed formula for the evaluation of $\mathfrak{sl}_N$-foams. URL: https://arxiv.org/abs/1702.04140.

[43] D.E.V. Rose and P. Wedrich. Deformations of colored $\mathfrak{sl}(n)$ link homologies via foams. *Geom. Topol.*, 20(6):3431–3517, 2016. URL: http://arxiv.org/abs/1501.02567, doi:10.2140/gt.2016.20.3431.

[44] L. Rozansky. An infinite torus braid yields a categorified Jones–Wenzl projector. *Fund. Math.*, 225(1):305–326, 2014. URL: https://arxiv.org/abs/1005.3266, doi:10.4064/fm225-1-14.

[45] A. Sartori and D. Tubbenhauer. Webs and q-Howe dualities in types **BCD**. URL: https://arxiv.org/abs/1701.02932.

[46] P. Vogel. Functoriality of Khovanov homology. URL: https://arxiv.org/abs/1505.04545.

[47] P. Wedrich. Exponential growth of colored HOMFLY–PT homology. URL: https://arxiv.org/abs/1602.02769.

[48] H. Wu. A colored $\mathfrak{sl}(N)$ homology for links in S^3. *Dissertationes Math. (Rozprawy Mat.)*, 499:217, 2014. URL: http://arxiv.org/abs/0907.0695, doi:10.4064/dm499-0-1.

[49] H. Wu. Equivariant colored $\mathfrak{sl}(N)$-homology for links. *J. Knot Theory Ramifications*, 21(2):1250012, 104, 2012. URL: http://arxiv.org/abs/1002.2662, doi:10.1142/S0218216511009558.

[50] Y. Yonezawa. Quantum $(\mathfrak{sl}_n, \wedge V_n)$ link invariant and matrix factorizations. *Nagoya Math. J.*, 204:69–123, 2011. URL: http://arxiv.org/abs/0906.0220.

M.E.: School of Mathematics & Statistics, Carslaw Building, University of Sydney, NSW 2006, Australia
E-mail address: michael.ehrig@sydney.edu.au

D.T.: Mathematisches Institut, Universität Bonn, Endenicher Allee 60, Room 1.003, 53115 Bonn, Germany
E-mail address: dtubben@math.uni-bonn.de

P.W.: Imperial College London, Department of Mathematics, 6M50 Huxley Building, South Kensington Campus London SW7 2AZ, United Kingdom
E-mail address: p.wedrich@imperial.ac.uk